

1 **Molecular analysis of long non-coding RNA GAS5 and microRNA-34a**
2 **expression signature in common solid tumors: A pilot study**

3 Eman A. Toraih^{1,2*}, Saleh Ali Alghamdi³, Aya El-Wazir^{1,2}, Marwa M Hosny⁴, Mohammad H.
4 Hussein⁵, Motaz S. Khashana⁶, Manal S. Fawzy^{4,7*}

5 ¹ Genetics Unit, Department of Histology and Cell Biology, Faculty of Medicine, Suez Canal
6 University, Ismailia, Egypt

7 ²Center of Excellence of Molecular and Cellular Medicine, Suez Canal University, Ismailia, Egypt

8 ³Medical Genetics, Clinical Laboratory Department, College of Applied Medical Sciences, Taif
9 University, Taif, Saudi Arabia

10 ⁴Department of Medical Biochemistry, Faculty of Medicine, Suez Canal University, Ismailia, Egypt

11 ⁵ Pulmonologist, Ministry of Health and Population, Cairo, Egypt

12 ⁶ Faculty of Medicine, Suez Canal University, Ismailia, Egypt

13 ⁷ Department of Biochemistry, Faculty of Medicine, Northern Border University, Arar, Saudi
14 Arabia.

15 ***Corresponding authors:**

16 E-mail: manal2_khashana@ymail.com (MSF)

17 E-mail: emantoraih@gmail.com (EAT)

18

19 **Short title:** LncRNA GAS5 and miR-34a expression in cancer

20

21

22

23

24

25

26

27 **Abstract**

28 Accumulating evidence indicates that non-coding RNAs including microRNAs (miRs) and long
29 non-coding RNAs (lncRNAs) are aberrantly expressed in cancer, providing promising biomarkers
30 for diagnosis, prognosis and/or therapeutic targets. We aimed in the current work to quantify the
31 expression profile of miR-34a and one of its bioinformatically selected partner lncRNA growth
32 arrest-specific 5 (*GAS5*) in a sample of Egyptian cancer patients, including three prevalent types of
33 cancer in our region; renal cell carcinoma (RCC), hepatocellular carcinoma (HCC) and
34 glioblastoma (GB) as well as to correlate these expression profiles with the available
35 clinicopathological data in an attempt to clarify their roles in cancer. Quantitative real-time
36 polymerase chain reaction analysis was applied. Different bioinformatics databases were searched
37 to confirm the potential miRNAs-lncRNA interactions of the selected ncRNAs in cancer
38 pathogenesis. *GAS5* was significantly under-expressed in the three types of cancer. However, levels
39 of miR-34a greatly varied according to the tumor type; it displayed an increased expression in RCC
40 [4.05 (1.003-22.69), $p < 0.001$] and a decreased expression in GB [0.35 (0.04-0.95), $p < 0.001$]. A
41 weak negative correlation was observed between levels of *GAS5* and miR-34a in GB [$r = -0.39$, p
42 $= 0.006$]. Univariate analyses revealed a correlation of *GAS5* downregulation with poor disease-
43 free survival ($r = 0.31$, $p = 0.018$) and overall survival ($r = 0.28$, $p = 0.029$) in RCC but not in GB,
44 and a marginal significance correlation with a higher number of lesions in HCC. Hierarchical
45 clustering analysis showed RCC patients among others, could be clustered by *GAS5* and miR-34a
46 co-expression profile. Our results confirm the tumor suppressor role of *GAS5* in cancer and suggest
47 its potential applicability to be a predictor of bad outcomes with other conventional markers for
48 various types of cancer. Further functional validation studies are warranted to confirm miR-
49 34a/*GAS5* interplay in cancer.

50

51 **Keywords:** *GAS5*; miR-34a; RCC; GB; HCC

52

53 **Introduction**

54 Cancer is now the second leading cause of mortality worldwide, causing 8.8 million deaths globally
55 in 2015, which is equivalent to one in every six deaths [1]. Cancer occurs as a net result of
56 activation of oncogenes and inhibition of tumor suppressor genes (TSGs) [2]. Decades back, it was
57 believed that oncogenes and TSGs had to code for proteins, and only mutations in protein-coding
58 genes would result in such pathological conditions as cancer. However, in the world of genetics, it
59 is never that simple. With the advancement of genetic technologies including next generation
60 sequencing, microarrays and bioinformatic machinery, many truths came to light, including what
61 was originally thought to be junk DNA is now found to code for thousands of equally significant
62 regulatory RNAs [3]. Since their discovery, the non-coding RNAs (ncRNAs) have been recognized
63 as epigenetic regulators of protein-coding genes. Recently, a whole new level of regulation has been
64 uncovered, when it was found that ncRNAs have the ability to regulate each other as well [4]
65 further adding to the complexity of the regulatory processes. This set of findings has revolutionized
66 our understanding of several human diseases, making this ‘the era of non-coding RNAs’.

67 Many classes of ncRNAs have been identified and linked to cancer, the most common of which are
68 micro RNAs (miRNAs), long-noncoding RNAs (lncRNAs), PIWI-interacting RNAs (piRNAs) and
69 small nucleolar RNAs (snoRNAs). The roles of these four types of ncRNAs in cancer are reviewed
70 in several studies [5-8]. In brief, overexpression of some ncRNAs as miRNAs or lncRNAs can
71 suppress the expression of TSG targets, while loss of function or reduced expression of others may
72 allow overexpression of the oncogenes they regulate. Furthermore, since each ncRNA may regulate
73 hundreds of different genes, its over or under expression may have widespread oncogenic effects
74 because many genes will be dysregulated [9].

75 Here we were interested in a relatively newly discovered lncRNA; Growth Arrest Specific 5
76 (GAS5) which is a poorly conserved gene mapped to chromosome 1q25.1 [10]. It consists of 12
77 exons and 11 introns from which 29 transcripts are produced from alternative splicing, many of
78 which contain retained introns (Ensembl Genome Browser 'GAS5'). The first two transcripts

79 discovered (produced from alternative splice sites on exon 7) are the GAS5a and GAS5b with the
80 latter being predominantly expressed in most cells [11]. Another synonym for the gene is ' Small
81 Nucleolar RNA Host Gene', this is for having the ability to produce multiple (10 in human) non-
82 coding small nucleolar RNAs (snRNAs) from its more conserved introns [11]. These snRNAs are
83 involved in the regulation of ribosomal RNA (rRNA) synthesis through 2-O-methylation of pre-
84 ribosomal RNA [12].

85 As its name implies, GAS5 is over expressed in growth-arrested cells [13]. This is further
86 demonstrated by the presence of high levels of GAS5 in brain cells, which are considered the
87 slowest dividing cells in the body as opposed to its lowest levels in other rapidly dividing cells, the
88 most important of which are cancer cells [14].

89 Expectedly, GAS5 under expression was found to be associated with multiple types of cancer [15-
90 25] and it was found to bind some miRNAs, including miR-21, miR-222 and miR-103 sponging
91 their inhibitory effect on their target TSGs ([16, 21, 26, 27].

92 Our bioinformatic analyses have revealed a potential new miRNA target for the GAS5 gene; miR-
93 34a. This miRNA is encoded from chromosome1p36.22. Its promotor is recognized for having
94 multiple CpG islands and a p53 binding site, making p53 a direct transcriptional regulator for this
95 miRNA [28, 29]. While the history of miR-34a with cancer is very well established, studies
96 conducted on different types of cancers have contradictory results regarding its actual role in tumor
97 progression. In other words, is it an oncogene or a TSG? Many studies have proved it's functioning
98 as a TSG in various types of cancer, including neuroblastoma [30], leukemia [31], pancreatic [32]
99 and hepatocellular [33, 34] carcinoma, glioblastoma (GB) [35, 36], breast [37] lung [38] and colon
100 [39] cancer. On the contrary, other studies have found that it functions as an oncogene through
101 promoting tumorigenesis as in RCC [40, 41], papillary thyroid carcinoma (PTC) [42], colon [39]
102 and uterine cancer [43]. It has been suggested that this discrepancy may be attributed to the tissue
103 type and the miR-34a/p53 pathway involved [41].

104 To the best of our knowledge, no clinical studies were conducted to explore both GAS5 and miR-

105 34a profiles in cancer patients. Hence, we were interested to investigate the expression profiles of
106 these ncRNAs in three prevalent types of cancer in our region; renal cell carcinoma (RCC),
107 hepatocellular carcinoma (HCC) and glioblastoma (GB) as well as to correlate these expression
108 profiles with the available clinicopathological data in an attempt to clarify their roles in cancer.

109 **Materials and Methods**

110 **Genomic characterization of GAS5 and miR-34a**

111 Chromosomal localization, genomic sequence and structure analysis, subcellular localization,
112 variant analysis, and folding pattern were retrieved from different online tools; including Ensembl
113 (<http://www.ensembl.org/>), GeneCards for human gene database (<http://www.genecards.org/>),
114 National Center for Biotechnology Information (NCBI) (ncbi.nlm.nih.gov/), COMPARTMENTS
115 subcellular localization (<https://compartments.jensenlab.org/Search>), Database of Transcription
116 Start Sites (DBTSS) version 10.0 (<http://dbtss.hgc.jp/>), KineFold (<http://kinfold.curie.fr/>), and
117 MFold webserver (<http://unafold.rna.albany.edu/?q=mfold/RNA-Folding-Form>).

118 **Exploring miR-34 and GAS5 interactions**

119 Identifying complementary regions between microRNA-34a and lncRNA GAS5 were demonstrated
120 by several tools; RNA22 microRNA target detection (<https://cm.jefferson.edu/rna22/>) and DIANA-
121 LncBase v2 (<http://diana.imis.athena-innovation.gr/DianaTools/index.php>).

122 **Functional enrichment analysis**

123 Pathway enrichment analysis and gene ontology of microRNA-34a was performed by Diana-
124 miRPath v3.0 (<http://diana.imis.athena-innovation.gr/DianaTools/index.php>) using its
125 experimentally validated gene targets. Functional enrichment analysis of GAS5 was obtained from
126 Ensembl and GeneCards databases to identify its biological function in cancer.

127 **Study population and sampling collection**

128 In total, 230 samples were analyzed, including 60 formalin-fixed, paraffin-embedded (FFPE) RCC
129 samples and their paired adjacent non-cancer tissues, 50 FFPE GB specimens and 10 non-cancer
130 brain tissues as well as 30 HCC blood samples and 20 controls.

131 **(a) RCC cohort**

132 The archived FFPE renal samples were taken from sixty patients who underwent radical
133 nephrectomy for a primary RCC and dating back for three years. All retrieved cases were archived
134 in the Pathology laboratory of Mansoura Oncology Center, Mansoura, Egypt. No history of
135 receiving neoadjuvant chemotherapy or radiotherapy prior to sampling. Clinicopathological data,
136 including the survival were collected from patient medical records. Paired sixty cancer-free adjacent
137 tissues were examined and sectioned to serve as controls for molecular analysis.

138 **(b) GB cohort**

139 Fifty glioblastoma patients and 10 non-cancer brain tissues collected from the archive of the
140 Pathology Department, Mansoura University Hospitals, Egypt, dating back for three years were
141 included in the current work. Detailed patients' data were retrieved from their follow up records.
142 They had GB grade 4, undergone surgical removal and had not received any treatment before
143 sampling. They followed-up for more than 3 years.

144 **(c) HCC cohort**

145 Following our local hospital and medical ethical committee rules in liver tissue sampling
146 prohibition from HCC patients, only blood samples were available. Thirty HCV-induced HCC and
147 20 matched controls from healthy blood bank donors were recruited in the study. Patients were
148 obtained from the outpatient clinic of Tropical Medicine and Gastroenterology Department, Faculty
149 of Medicine, Assuit, Egypt. They had typical imaging findings of liver cancer and elevated alpha
150 fetoprotein (AFP). Patients underwent clinical and radiological assessment, confirmation of HCV
151 by PCR, Barcelona-Clinic Liver Cancer (BCLC) staging, and Child-Turcotte-Pugh (CTP) scoring
152 (44). Survival data for HCC patients were not available in patients' medical records. Hence, these
153 data were not included in the statistical analysis for HCC patients.

154 **Ethical approval**

155 The study was conducted according to the ethical guidelines of the Declaration of Helsinki and
156 approved by the Medical Research Ethics Committee of Suez Canal University.

157 **RNA extraction**

158 Total RNA; including the small RNA, was isolated from either FFPE tissue sections (5 to 8- μ m-
159 thick) using the Qiagen miRNeasy FFPE Kit (*Qiagen, cat no 217504*) or serum using Qiagen
160 miRNeasy serum/plasma Kit (*Qiagen, cat no 217184*) following the protocols supplied by the
161 manufacturer. Concentration of RNA was determined using the NanoDrop ND-1000
162 spectrophotometer (*NanoDrop Tech., Inc. Wilmington, DE, USA*). Samples with a 260/280 nm
163 absorbance ratio less than 1.8 were excluded.

164 **Reverse transcription reaction**

165 Subsequently, RNA for lncRNA GAS5 was converted to complementary DNA (cDNA) in a T-
166 Professional Basic, Biometra PCR System (*Biometra, Goettingen, Germany*) using high Capacity
167 cDNA Reverse Transcription Kit (*Applied Biosystems, P/N 4368814*) with RT random primers as
168 previously described [45].

169 Reverse transcription of miR-34a was specifically converted to cDNA using TaqManTM MicroRNA
170 Reverse Transcription kit (*P/N 4366596; Applied Biosystems, Foster City, CA, USA*) with 5x
171 miRNA specific stem-loop primers as previously described in our prior publication [46].
172 Appropriate controls were included in each experiment.

173 **LncRNA GAS5 and microRNA-34a expression analyses**

174 The Real-Time PCR reactions were performed in accordance with the Minimum Information for
175 Publication of Quantitative Real-Time PCR Experiments (MIQE) guidelines [47]. The expression
176 level of *GAS5* was assessed via SYBR Green qPCR analysis and normalized with GAPDH. The
177 following primers were designed using Primer 3 software and checked by *in silico* PCR
178 amplification of the University of California, Santa Cruz (UCSC) genome browser; for *GAS5*:
179 Forward: 5'- CTTGCCTGGACCAGCTTAAT-3'; Reverse: 5'-CAAGCCGACTCTCCATACCT-
180 3', and for *GAPDH*: Forward: 5'- CGGATTTGGTCGTATTGGG-3'; Reverse: 5'-
181 CTGGAAGATGGTGTGATGGGATT-3'. In brief, 10 μ l of qPCR Green Master (*Jena Bioscience,*
182 *Cat no. PCR-313L*), 0.6 μ l (10 μ M) forward and reverse primers, 8 μ l PCR grade water, and 1 μ l

183 cDNA template were included in the reaction for *GAS5* and *GAPDH* SYBR Green assay
184 analyses [46]. For microRNA quantification, a final volume of 20 μ l was adjusted in duplicate,
185 including 1.33 μ l specific RT products, 2 \times TaqMan[®] Universal PCR Master Mix with UNG
186 (Applied Biosystems, P/N 4440043), and 20 \times of 1 μ l specific TaqMan[®] RNA assay for hsa-miR-
187 34a-5p (Applied Biosystems, assay ID 000426) and Taqman[®] Universal PCR master mix II, No
188 UNG (2 \times) [48]. Two endogenous control assays were used; TATA box binding protein (TBP; assay
189 ID Hs00427620_m1) in brain cancer and RNU6B (assay ID Hs001093) in liver and renal cancer
190 [49, 50]. Appropriate negative and positive controls were used. The PCR for 96-well plates was
191 carried out using StepOne[™] Real-Time PCR System (Applied Biosystem) and incubated as
192 follows: 95 $^{\circ}$ C for 10 min followed by 45 cycles of 92 $^{\circ}$ C for 15 seconds and 60 $^{\circ}$ C for 1 minute. Ten
193 percent randomly selected study samples were re-evaluated in separate runs for the study gene
194 expressions to test the reproducibility of the qPCR which showed very close quantitative cycles
195 value results and low standard deviations.

196 **Statistical analysis**

197 R package (version 3.3.2) and Statistical Package for the Social Sciences (SPSS) for Windows
198 software (version 22.0) were used for data analyses. Categorical variables were compared using
199 the Chi-square (χ^2) or Fisher's exact tests where appropriate. Wilcoxon matched-pair signed-rank
200 and Mann-Whitney U tests were used for tissues of renal/brain cancer and serum of liver cancer
201 patients, respectively, to compare continuous variables. The correlation between miR-34a level
202 and *GAS5* expressions was calculated by Spearman's rank correlation analysis. A two-tailed *p*-
203 value of < 0.05 was considered statistically significant. The receiver operating characteristic (ROC)
204 curves were performed to get the best cutoff values of miRNA-34a for discriminating long and
205 short survivors in cancer patients. The fold change of ncRNAs expressions in each patient relative
206 to the control was calculated via Livak method based on the quantitative cycle (C_q) values with the
207 following equation: relative quantity = $2^{-\Delta\Delta C_q}$; where $\Delta\Delta C_q = (C_q \text{ ncRNA} - C_q \text{ internal control})_{\text{cancer}}$
208 $- (C_q \text{ ncRNA} - C_q \text{ internal control})_{\text{control}}$ [51]. Univariate analysis for association between ncRNA

209 expression profile and clinico-pathological features in cancer patients was run. The software
210 package named PC-ORD ver. 6 [52] was employed to run different multivariate analyses for
211 clustering analysis of patients according to clinico-pathological and molecular data.

212 **Results**

213 **Genomic location of GAS5**

214 Lnc-RNA GAS5 is also known as small nucleolar RNA host gene 2 (SNHG2) and non-protein
215 coding RNA 30 (NCRNA00030). It is encoded by GAS5 gene on chromosome 1q25.1 (Genomic
216 coordination at 1:173863901-173867987 at the negative strand according to human genome
217 assembly GRCh38) (**Fig. 1A**). It consists of 12 exons, spanning 4.087 kb and encoding for 29
218 different alternative splice transcripts ranging in length from 242 to 1698 bp (Electronic
219 Supplementary Table S1).

220 **Sequence analysis of GAS5**

221 *GAS5* gene contains a seven-nucleotide oligo-pyrimidine tract on its 5'-end in exon 1, hence is
222 classified as a member of the 5' terminal oligo-pyrimidine (TOP) genes. This sequence can act as a
223 cis-regulatory motif which either inhibits the binding of translational regulatory proteins
224 downstream to the transcriptional start sites of mRNAs or suppresses the translational machinery
225 itself. In addition to its translational controls, the TOP elements are known to modulate gene
226 expression through regulating transcription [53]. Being one of the TOP genes, it is ubiquitously
227 expressed and is predicted to regulate the translation of more than 20% of total mRNAs [DataBase
228 of Transcription Start Sites]

229 Sequence analysis of *GAS5* gene revealed that it is a small nucleolar RNA host gene, containing
230 multiple *snoRNA* genes within its introns. These genes encode for ten C/D box snoRNAs, which
231 contain the C (UGAUGA) and D (CUGA) box motifs. They are predicted to play a role in the 2'-O-
232 methylation of rRNA by guiding guanine methylation, which enhances RNA folding and
233 interaction with ribosomal proteins. *GAS5* also hosts SNORDA103 within intron 4, an H/ACA box
234 snoRNA, which is associated with pseudouridylation (**Fig. 1B**).

235 **Variant analysis**

236 *GAS5* gene is shown to be highly polymorphic, enclosing around 300 thousand variants (75%
237 intronic, 21% exonic, and 4% splice region polymorphisms). Among all these polymorphisms, 14
238 SNPs, one deletion and one insertion are common variants with minor allele frequency (MAF) >
239 0.05 (**Fig. 1C**) and (Electronic Supplementary Table S2).

240

241 **Fig. 1 Structural analysis of *GAS5* gene.** (A) Chromosomal localization of *GAS5* gene. It is
242 present on chromosome 1q25.1, at genomic coordination 1:173863901-173867987 on the negative
243 strand (according to human genome assembly GRCh38). (B) Sequence analysis of *GAS5* gene. It
244 consists of 12 exons, spanning 4.087 kb that code for 29 different alternative splice transcripts. It
245 hosts multiple snoRNA genes within its introns (except intron 9). These genes encode for ten C/D
246 box snoRNAs, which contain the C (UGAUGA) and D (CUGA) box motifs, and an H/ACA box
247 snoRNA, SNORDA103, within intron 4. (C) Genetic variant analysis. *GAS5* gene (4087 bases long)
248 contains around 300 thousand variants (75% intronic, 21% exonic, and 4% splice region
249 polymorphisms). Among all these polymorphisms, 14 SNPs (red), one deletion (green) and one
250 insertion (blue) are common variants with minor allele frequency (MAF) > 0.05. (D) Subcellular
251 localization of lncRNA *GAS5*. Text mining highlighted its predominant existence intranuclear and
252 within extracellular exosomes which are extruded into the circulation. (F) Folding pattern of
253 lncRNA *GAS5*. [Data source: Ensembl.org, genecards.org, NCBI, COMPARTMENT database, and
254 MFold]

255

256 ***GAS5*-miRNA interaction**

257 Analysis with the RNA22 program (<http://cbcsrv.watson.ibm.com/rna22.html>) identified
258 complementary regions of *GAS5* with 690 microRNAs. Among these putative microRNAs, only
259 252 interactions with 234 microRNAs showed significant binding ($p < 0.05$) (Electronic
260 Supplementary Table S3). Via DIANA-LncBase v2 database for experimentally validated miRNA-

261 lncRNA interactions, GAS5 was identified as a miR-34a target by immunoprecipitation
262 experiments (score=0.558). For further confirmation, we used RNA22 software to determine the
263 interaction binding sites between GAS5 transcripts and miR-34a. Our results showed base-pairing
264 in twenty-three alternative splice variants. Among them, nine transcripts had two miR-34a binding
265 sites (Electronic Supplementary Table S4).

266 **miR-34a functional analysis**

267 Hundreds of miR-34a-5p and 3p targets were retrieved from various online databases; including
268 miRTarBase (<http://mirtarbase.mbc.nctu.edu.tw/>), miRDB (<http://mirdb.org/>) and microRNA.org.
269 Functional enrichment analysis revealed its enrollment in cancer-related KEGG pathways, as
270 Pathways in cancer (hsa05200, 115 targets, $p=0.001723304$), proteoglycans in cancer (hsa05205, 71
271 targets, $p=1.687731e-06$), adherens junction (hsa04520, 34 targets, $p = 3.396929e-06$), cell cycle
272 (hsa04110, 54 targets, $p = 3.355808e-05$), and p53 signaling pathway (hsa04115, 31 targets, $p =$
273 0.006060223) as well as cancer-specific pathways, namely glioma (hsa05214, 29 targets, $p =$
274 0.0003111577) and renal cell carcinoma (hsa05211, 28 targets, $p= 0.02521455$) (Electronic
275 Supplementary Table S5). GO analysis (Diana tools) demonstrated miR-34a to be involved in cell
276 death, cell cycle, and response to stress thus highlighting its role in cancer cell growth. In addition,
277 miR-34a was significantly associated with membrane organization, cell junction organization, and
278 cell motility, hence may play a key role in cancer cell invasion and metastasis (**Fig. 2**).

279

280 **Fig. 2 Functional and structural analysis of miR-34a.** (A) GAS5: miR-34a-5p interaction.
281 Complementarity regions are shown in three binding sites in *GAS5* gene, one proximal at 5' region
282 (1432-1455) and two distal at 3' end (3545-3567 and 3698-3719) [Data source: RNA22, DIANA-
283 LncBase v2]. (B) Predicted secondary structure of miR-34a. Folding pattern and energy are
284 demonstrated [Data source: KineFold]. (C) Functional enrichment analysis of miR-34a
285 experimentally validated gene targets. Significant clustered heat map represents the gene ontology
286 using GO slim option, FDR conservative states, p value threshold < 0.05 , and categories union

287 [Data source: DIANA-miRPath v3]. <http://snf-515788.vm.oceanos.grnet.gr/uploads/R/HeatMap290913.png>

289

290 Characteristics of the study population

291 Baseline characteristics of RCC, GB, and HCC cohorts are demonstrated in **Tables 1 to 3**.

292 **Table 1. Clinicopathological characteristics of renal cell carcinoma patients**

293

Variables	Total	Low OS	High OS	<i>p</i> value
Total number	60 (100)	19 (31.7)	41 (68.3)	
Age				
≤55 years	6 (10.0)	3 (15.8)	3 (7.3)	0.370
>55 years	54 (90.0)	16 (84.2)	38 (92.7)	
Gender				
Female	21 (35.0)	9 (47.4)	1 (29.3)	0.245
Male	39 (65.0)	10 (52.6)	29 (70.7)	
HPD				
Clear cell	30 (50.0)	8 (42.1)	22 (53.7)	0.354
Papillary	15 (25.0)	4 (21.1)	11 (26.8)	
Chromophobic	15 (25.0)	7 (36.8)	8 (19.5)	
Tumor location				
Right side	22 (36.7)	7 (36.8)	15 (36.6)	0.985
Left side	38 (63.3)	12 (63.2)	26 (63.4)	
Grade				
Grade 1	9 (15.0)	1 (5.3)	8 (19.5)	0.023
Grade 2	28 (46.7)	6 (31.6)	22 (53.7)	
Grade 3	23 (38.3)	12 (63.2)	11 (26.8)	
Tumor size				
T1	21 (35.0)	6 (31.6)	15 (36.6)	0.589
T2	25 (41.7)	7 (16.8)	18 (43.9)	
T3	14 (23.3)	6 (31.6)	8 (19.5)	
LN				
Negative	39 (65.0)	11 (57.9)	28 (68.3)	0.562
Positive	21 (35.0)	8 (42.1)	13 (31.7)	
Recurrence				
Negative	44 (73.3)	7 (36.8)	37 (90.2)	<0.001
Positive	16 (26.7)	12 (63.2)	4 (9.8)	
DFS				
≤ 1year	29 (48.3)	19 (100)	10 (24.4)	<0.001
> 1year	31 (51.7)	0 (0.0)	31 (75.6)	
GAS5 fold				
≤ 1-fold	55 (91.7)	19 (100)	36 (87.8)	0.283
> 1-fold	3 (5.0)	0 (0.0)	3 (7.3)	
>10-folds	2 (3.3)	0 (0.0)	2 (4.9)	

miR-34a fold				
≤ 1-fold	15 (25.0)	6 (31.6)	9 (22.0)	0.192
> 1-fold	19 (31.7)	8 (42.1)	11 (26.8)	
>10-folds	26 (43.3)	5 (26.3)	21 (51.2)	

294 *HPD* histopathological diagnosis, *DFS* disease-free survival, *OS* overall survival. Low OS: ≤12
 295 months, High OS: >12 months. Fisher's Exact and Pearson Chi-square tests were used. Bold values
 296 indicate statistical significance at $p < 0.05$

297

298 **Table 2. Clinicopathological characteristics of glioblastoma patients**

Variables	Total	Low OS	High OS	<i>p</i> value
Total number	50 (100)	10 (20.0)	40 (80.0)	
Age				
≤55 years	21 (42.0)	7 (70.0)	14 (35.0)	0.073
>55 years	29 (58.0)	3 (3.0)	26 (65.0)	
Gender				
Female	13 (26.0)	1 (10.0)	12 (30.0)	0.258
Male	37 (74.0)	9 (90.0)	28 (70.0)	
Tumor location				
Frontal	24 (48.0)	8 (80.0)	16 (40.0)	0.071
Temporo-paroetal	18 (36.0)	1 (10.0)	17 (42.5)	
Fronto-temporal	8 (16.0)	1 (10.0)	7 (17.5)	
Recurrence				
Negative	44 (88.0)	8 (80.0)	36 (90.0)	0.586
Positive	6 (12.0)	2 (20.0)	4 (10.0)	
DFS				
≤ 1year	25 (50.0)	10 (100)	15 (37.5)	0.001
> 1year	25 (50.0)	0 (0.0)	25 (62.5)	
GAS5 fold				
≤ 1-fold	37 (74.0)	7 (70.0)	30 (75.0)	0.707
> 1-fold	13 (26.0)	3 (30.0)	10 (25.0)	
>10-folds				
miR-34a fold				
≤ 1-fold	38 (76.0)	8 (80.0)	30 (75.0)	0.741
> 1-fold	12 (24.0)	2 (20.0)	10 (25.0)	
>10-folds	0 (0.0)			

299 Data are presented as number (frequency). *HPD* histopathological diagnosis, *DFS* disease-free
 300 survival, *OS* overall survival. Low OS: ≤12 months, High OS: >12 months. Fisher's Exact and
 301 Pearson Chi-square tests were used. Bold values indicate statistical significance at $p < 0.05$

302 **Table 3. Clinicopathological characteristics of hepatocellular carcinoma patients**

Variables	Patients (n=30)
Total number	
Age	
≤55 years	13 (43.3)
>55 years	17 (56.7)
Gender	
Female	11 (36.7)
Male	19 (63.3)
Tumor size	
<5 cm	9 (30.0)
≥5 cm	21 (70.0)
Number of lesions	
Solitary	20 (66.7)
Multiple	10 (33.3)
LCF score	9.7±1.2
CTP class	
Child B	21 (70.0)
Child C	9 (30.0)
Hepatomegaly	
Mild	18 (60.0)
Massive	12 (40.0)
Treatment	
Ablation	15 (30.0)
Radiofrequency	11 (36.7)
Supportive	4 (13.3)
GAS5 fold	
≤ 1-fold	27 (90.0)
> 1-fold	3 (10.0)
miR-34a fold	
≤ 1-fold	19 (63.3)
> 1-fold	10 (33.3)

303 Data are presented as number (frequency). *CTP* Child-Turcotte-Pugh classification for liver cell
 304 failure, *LCF* liver cell failure score by *CTP* classification. Fisher's Exact and Pearson Chi-square
 305 tests were used.

306

307 **Expression profiling**

308 GAS5 levels were under-expressed in RCC [0.08 (0.006-0.38), $p < 0.001$], GB [0.10 (0.003-0.89), p
 309 < 0.001] and HCC [0.12 (0.015-0.74), $p < 0.001$]. On the other hand, miR-34a displayed an
 310 increased expression in RCC [4.05 (1.003-22.69), $p < 0.001$] and a decreased expression in GB
 311 [0.35 (0.04-0.95), $p < 0.001$] as depicted in **Fig. 3**. A weak negative correlation was observed
 312 between levels of GAS5 and miR-34a in GB [$r = -0.39$, $p = 0.006$] (**Fig. 4**).

313

314 **Fig. 3 Relative expression of GAS5 and miR-34a-5p in cancer.** *RCC* renal cell carcinoma, *GB*
315 glioblastoma, *HCC* hepatocellular carcinoma. Data are represented as medians. The box defines
316 upper and lower quartiles (25% and 75%, respectively) and the error bars indicate upper and
317 lower adjacent limits. Expression levels in cancer and control samples were normalized to
318 GAPDH in RCC and HCC, TBP in GB and RNU6B for microRNA and calculated using the
319 delta-delta CT method [$= 2^{-\Delta\Delta CT}$] in comparison to controls. Fold change of controls were
320 set at 1.0. Wilcoxon matched-pair signed-rank and Mann-Whitney U tests were used for tissues
321 of renal/brain cancer and serum of liver cancer patients, respectively. Two-sided $p < 0.05$ was
322 considered statistically significant

323

324 **Fig. 4 Correlation between GAS5 and miR-34a-5p expression levels.** *RCC* renal cell carcinoma,
325 *GB* glioblastoma, *HCC* hepatocellular carcinoma. Spearman's rank correlation test was used.
326 Statistical significance was considered at $p < 0.05$.

327

328 **Association of GAS5 and miR-34a with clinicopathological features**

329 Univariate analyses are shown in **Table 4A**, B, and C. The lower GAS5 level was correlated
330 with poor DFS ($r = 0.31$, $p = 0.018$) and OS ($r = 0.28$, $p = 0.029$) in RCC but not in GB, and was
331 correlated by a marginal significance ($r = -0.35$, $p = 0.056$) with a higher number of lesions in
332 HCC. Levels of miR-34a did not correlate with any clinico-pathological features.

333

334

335

336

337

338

339 **Table 4. Univariate analysis for association between gene profile and clinico-pathological**
 340 **features in the study cohorts**

	(a) RCC			
	GAS5		miR-34a	
	<i>p</i> _{ass}	<i>r</i> (<i>p</i> _{corr})	<i>p</i> _{ass}	<i>r</i> (<i>p</i> _{corr})
Age	0.239	-0.069 (0.598)	0.352	-0.066 (0.619)
Gender	0.631	0.063 (0.635)	0.798	-0.033(0.801)
Location	0.908	-0.015 (0.910)	0.884	0.019 (0.886)
HPD	0.257	0.191 (0.143)	0.504	-0.130(0.321)
Grade	0.402	0.171 (0.192)	0.378	-0.167 (0.204)
Tumor size	0.199	0.157 (0.230)	0.361	-0.152 (0.246)
LN	0.193	0.169 (0.195)	0.258	-0.147(0.261)
Recurrence	0.192	0.170 (0.195)	0.371	-0.116 (0.376)
DFS	0.120	0.305 (0.018)	0.363	0.215 (0.099)
OS	0.266	0.283 (0.029)	0.441	0.191 (0.144)
	(b) GBM			
Age	0.883	0.063 (0.663)	0.930	-0.013 (0.931)
Gender	0.921	-0.014 (0.922)	0.514	-0.093 (0.520)
Location	0.530	-0.150 (0.300)	0.711	0.091 (0.531)
Recurrence	0.258	0.166 (0.248)	0.070	-0.260 (0.068)
DFS	0.869	0.012 (0.936)	0.677	0.074 (0.609)
OS	0.451	0.48 (0.743)	0.356	0.013 (0.927)
	(c) HCC			
Age	0.869	-0.037 (0.848)	0.059	-0.289 (0.121)
Gender	0.553	0.112 (0.556)	0.420	0.156 (0.411)
Hepatomegaly	0.692	-0.079 (0.680)	0.851	0.039 (0.837)
Tumor size	0.226	0.278 (0.137)	0.209	-0.315 (0.090)
Number of lesions	0.193	-0.352 (0.056)	0.916	0.112 (0.225)
CTP class	0.283	-0.206 (0.275)	0.533	0.122 (0.521)
Treatment	0.715	0.144 (0.447)	0.598	0.006 (0.973)

341 *p*_{ass} *p* values for association, *r* (*p*_{corr}) correlation spearman's coefficient and *p* value of
 342 correlation, *HPD* histopathological diagnosis, *T* tumor size, *LN* lymph node, *DFS* disease-free
 343 survival, *OS* overall survival, *CTP* Child-Turcotte-Pugh classification for liver cell failure.
 344 Spearman's rank, Mann-Whitney U and Kruskal-Wallis tests were used. Statistically significant
 345 values (*p* < 0.05) are shown in bold.

346
 347

348 **Role of GAS5 and miR-34a as markers of cancer prognosis**

349 ROC curves showed no prognostic value for GAS5 nor miR-34a to predict survival of cancer
 350 patients in RCC and GB, or to predict CTP class for liver cell failure in HCC patients (*p* > 0.05)

351 **(Fig. 5).**

352

353 **Fig. 5 Receiver Operating Characteristics (ROC) analysis for the prognostic value of markers.**

354 *RCC* renal cell carcinoma, *GB* glioblastoma, *HCC* hepatocellular carcinoma, *AUC* area under
355 curve, *CTP* Child-Turcotte-Pugh classification for liver cell failure

356

357 **Survival analysis in RCC and GB**

358 In RCC, multivariable analysis using logistic regression test (Enter method) showed age and
359 pathological grade to be independent predictors for recurrence: (OR = 1.251, 95% CI = 1.075-
360 1.455, $p = 0.004$) for the age and (OR = 19.9, 95% CI = 1.034-383, $p = 0.047$) for the grade.

361 Kaplan-Meier curve analysis and log-rank test revealed that RCC patients with female gender, post-
362 nephrectomy recurrence, advanced pathological grade, and down-regulated miR-34a levels had
363 significantly poor overall survival than their corresponding ($p < 0.05$) (**Table 5**). In addition,
364 multivariable analysis by Cox regression model demonstrated gender and recurrence to be
365 independent predictors of overall survival (hazard ratio (HR)=2.49; 95 % confidence interval
366 (95 % CI) 1.14–5.41, $p = 0.021$) and (HR = 4.16; 95% CI of 1.88–9.16, $p < 0.001$), respectively.

367 In GB, Kaplan-Meier curves showed a significant association of shorter survival times with male
368 gender (Breslow test: $p = 0.002$ and Tarane-Ware test: $p = 0.030$). In addition, marginal
369 significance was observed for poor overall survival in patients with frontal lesions (Log rank test: p
370 = 0.050) (**Table 6**). Multivariable analysis by Cox regression model illustrated tumor recurrence to
371 be an independent predictor of low overall survival (HZ = 11.1; 95 % CI 2.88-42.5, $p < 0.001$).

372

373

374

375

376

377

378
379
380

Table 5. Multivariable analysis in renal cell carcinoma patients

Variables	Survival time OS (mo)	Overall comparisons			Cox regression	
		Log Rank	Breslow	Tarone-Ware	HR (95% CI)	<i>p</i>
Age						
≤55 years	13.1 ± 2.22					
>55 years	16.1 ± 0.8	0.186	0.244	0.221	0.97 (0.92-1.01)	0.217
Gender						
Female	13.9 ± 1.28					
Male	16.7 ± 0.94	0.027	0.077	0.095	2.49 (1.14-5.41)	0.021
HPD						
Type 1	16.1 ± 1.12					
Type 2	17.5 ± 1.61				0.70 (0.34-1.46)	0.351
Type 3	13.3 ± 1.25	0.103	0.198	0.159	0.69 (0.30-1.60)	0.397
Location						
Right side	16.3 ± 1.23					
Left side	15.4 ± 1.00	0.703	0.489	0.539	1.08 (0.57-2.06)	0.807
Grade						
Grade 1	16.3 ± 1.53					
Grade 2	18.0 ± 1.17					
Grade 3	12.8 ± 1.05	0.005	0.003	0.003	1.60 (0.66-3.85)	0.293
Tumor size						
T1	16.4 ± 1.40					
T2	15.9 ± 1.13				0.91 (0.30-2.75)	0.871
T3	14.5 ± 1.65	0.709	0.577	0.635	0.89 (0.34-2.29)	0.813
LN						
Negative	16.4 ± 0.97					
Positive	14.6 ± 1.27	0.306	0.235	0.255	1.05 (0.42-2.59)	0.911
Recurrence						
Negative	17.5 ± 0.83					
Positive	10.8 ± 1.07	<0.001	<0.001	<0.001	4.16 (1.88-9.16)	<0.001
GAS5 fold						
Under-expressed	15.7 ± 0.84					
Over-expressed	16.2 ± 1.24	0.735	0.753	0.985	0.29 (1.04-0.96)	0.291
miR-34a fold						
Under-expressed	13.2 ± 0.99					
Over-expressed	16.6 ± 0.95	0.010	0.049	0.024	1.001 (0.98-1.01)	0.926

381 Survival times is shown as mean and standard error, *OS* overall survival, *HR (95% CI)* Hazard
382 ratio (95% confidence interval), *HPD* histopathological diagnosis, *T* tumor size, *LN* lymph node,
383 Statistically significant values ($p < 0.05$) are shown in bold.

384
385

386

387

388

389

390

391
392

Table 6. Multivariable analysis in glioblastoma patients

Variables	Survival time	Overall comparisons			Cox regression	
	OS (mo)	Log Rank	Breslow	Tarone-Ware	HR (95% CI)	<i>p</i>
Age						
≤55 years	17.8 ± 1.4	0.742	0.683	0.595	1.03 (0.97-1.09)	0.298
>55 years	17.0 ± 0.96					
Gender						
Female	20.5 ± 1.5	0.096	0.002	0.030	1.36 (0.45-4.11)	0.583
Male	16.2 ± 0.8					
Tumor location						
Frontal	15.7 ± 1.01	0.050	0.079	0.062		0.749
Temporo-paroetal	17.6 ± 1.3				1.3 (0.53-3.39)	0.534
Fronto-temporal	21.5 ± 2.1				1.5 (0.44-5.75)	0.472
Recurrence						
Negative	17.6 ± 0.8	0.284	0.397	0.342	11.1 (2.88-42.5)	<0.001
Positive	15.3 ± 1.8					
GAS5 fold						
Under-expressed	17.5 ± 0.9	0.765	0.581	0.642	0.96 (0.49-1.85)	0.904
Over-expressed	16.9 ± 1.6					
miR-34a fold						
Under-expressed	17.7 ± 0.9	0.460	0.453	0.415	1.14 (0.79-1.65)	0.471
Over-expressed	16.1 ± 1.5					

393
394
395
396

Survival time is shown as mean and standard error, *OS* overall survival, *HR (95% CI)* Hazard ratio (95% confidence interval). Statistically significant values ($p < 0.05$) are shown in bold.

397 Hierarchical clustering analysis

398 Dendrograms for Two-way agglomerative hierarchical cluster analysis, were employed (**Fig. 6**).
399 The following cluster setup parameters were adjusted: Distance method: Sorensen (Bray-Curtis),
400 Group Linkage Method: Flexible Beta at 0.75, Clustering of factor relative by factor maximum. A
401 distance matrix is shown. RCC plot analyzed 60 strands and 12 factors, GB plot analyzed 50 strands
402 and 9 factors, whereas HCC dendrogram showed results of 30 strands and 11 factors. Clustering
403 analysis revealed separation of RCC patients by GAS5 and miR-34a levels, GB patients by survival
404 times, and HCC patients by their age.

405
406
407

408 **Fig. 6 Multivariate analysis of patients according to combined transcriptomic signature of**
409 **genes and clinicopathological features. (A) RCC, (B) GB, (C) HCC.** RCC patients were divided
410 based on GAS5 and miR-34a levels, GB patients were divided by survival times, and HCC patients
411 by age

412

413 Discussion

414 In this study, we measured the expression of two ncRNAs; the lncRNA GAS5 and the miRNA
415 miR-34a in three of the most prevalent and high-incidence tumors in Egypt; hepatic, renal and brain
416 cancer. We chose more than one tumor type to assess if the same ncRNA could work differently
417 according to the tissue type. We also investigated the possible association between GAS5 and miR-
418 34a in mediating carcinogenesis after detecting an interaction between the two through our
419 preliminary *in silico* analysis.

420 Our results show that *GAS5* was under-expressed in the three types of cancer; RCC, HCC and GB.
421 On the other hand, levels of miR-34a greatly varied according to the tumor type. RCC patients had
422 a lower *GAS5* level and a higher miR-34a level in tumor tissue compared to adjacent normal tissue.
423 Moreover, *GAS5* levels were correlated with poor survival. In accordance, Qiao et al. reported a
424 reduced *GAS5* level in RCC cell lines compared to normal cell lines. Furthermore, *in vitro* cloning
425 and functional expression analysis revealed that *GAS5* overexpression caused cell cycle arrest,
426 increased apoptosis, as well as inhibited tumor metastatic potential [24], which could explain the
427 correlation between reduced patient survival and *GAS5* level in our study. As for miR-34a, several
428 studies reported over-expression of this RNA in RCC patients [40, 41, 54-56]. Liu et al. predicted
429 that its oncogenic function could be through targeting the two tumor suppressors secreted frizzled
430 related protein 1 (SFRP1) and calmodulin binding transcription activator 1 (CAMTA1), and further
431 validated the first target [40]. Another study noticed that miR-34a enhances cell survival, both in
432 *in vitro* and *in vivo* during cisplatin nephrotoxicity through p53 [57]. Collectively, the previous studies
433 suggest that miR-34a can act as an oncogene in renal tissue. On the contrary, Yadav et al. detected

434 a significant under-expression of miR-34a in both sera and renal tissues of RCC patients [58].
435 Similar results were demonstrated by the studies of Zhang et al. and Weng et al. [59, 60], where the
436 former study demonstrated that decreased expression of miR-34a in RCC patients inversely up-
437 regulated the gene for the transcription factor YY1. The latter study suggested that under-
438 expression of miR-34a in cancer tissues of RCC patients affected the regulation of the *NOTCH1*
439 gene, as well as caused dysregulation of other multiple miR-34a targets in 786-O and Caki-1 RCC
440 cell lines. Yu et al. found that miR-34a suppressed tumor growth and metastasis in *vivo* and in *vitro*
441 through targeting CD44 [61]. Another study found that miR-34a inhibits cellular invasion in renal
442 cancer cell lines A498 and 769P through targeting the 3' untranslated region (UTR) of the *c-myc*
443 oncogene [62]. Also, the lncRNA NEAT1 (nuclear paraspeckle assembly transcript 1) was found to
444 sponge miR-34a releasing its inhibition on the *c-met* oncogene, resulting in increased cellular
445 proliferation and invasion in RCC cell lines 786-O and ACHN [63]. Furthermore, Bai et al. found
446 that miR-34a causes senescence of rat renal cells through targeting two anti-oxidative mitochondrial
447 genes [64]. Cellular senescence, which is an irreversible state of growth arrest, protects the cells
448 from accumulating mutations that could lead to malignant transformation [65]. Further supporting
449 the tumor suppressor potential of miR-34a, Zhou et al. provided evidence that miR-34a, secreted by
450 fibroblasts, enhances apoptosis of renal tubular cells through regulating the anti-apoptotic gene
451 *BCL-2* [66].

452 The inconsistent results between our study which shows up-regulation of *miR-34a* in RCC and
453 other studies showing its under-regulation in the same type of cancer could have many possible
454 explanations. First, we measured the expression of miR-34a in cancer tissues obtained directly from
455 RCC patients as opposed to other studies conducted on cancer cell lines. While those cell lines are
456 highly essential for functional molecular analysis, they may be different from primary tumors,
457 possibly through building up new mutations in their attempt to adjust to their artificial environment
458 [67, 68]. Such mutations may easily alter cellular responses and regulatory mechanisms, possibly
459 affecting the expression of *miR-34a*. Second, miR-34a could be a non-specific molecule that can

460 both activate or inhibit tumorigenesis depending on the surrounding environment. These include
461 internal stimuli (other regulatory molecules or polymorphisms, oxidative molecules, other
462 associated disease states, tumor stage/grade or else) and external stimuli (cellular response to
463 environmental exposures, including chemotherapy, other drugs, chemicals, foods, etc). Third, miR-
464 34a has multiple targets (discussed in our previous work) [41], as well as being itself a target for
465 many lncRNAs. Each study focuses on one or few targets, and infers a tumor suppressor or an
466 oncogenic function based on its effect on the studied target/pathway. However, miR-34a is one
467 small molecule in a larger network of molecules that either promotes or inhibits tumorigenesis
468 based on the net result of *all* its regulated targets, which could easily differ according to countless
469 variables. Given by the negative correlation of this microRNA with GAS5 in our RCC patients, as
470 well as the predicted interaction between the two, we believe that a new pathway; the *GAS5*/miR-
471 34a pathway might be involved in the previously indicated molecular network leading to RCC.

472 The interaction between lncRNAs and miRNAs can be multifaceted. Yoon et al. explained four
473 mechanisms of interaction between the two types [69]. First, lncRNAs can act as miRNA sponges
474 as previously mentioned with examples in the introduction. Second, the opposite can occur, where
475 miRNAs can inhibit lncRNAs by binding to them and causing their degradation. This applies for
476 miR145-5p, miR-181a-5p and miR-99b-3p which inhibit lncRNA ROR [70], and miR-9 which
477 inhibits lncRNA MALAT1 [71]. Third, miRNAs and lncRNAs can both compete for the same
478 binding site on mRNAs, an example of which is miR-485-5p and lncRNA BACE1AS competing
479 for BACE1 mRNA [72]. Fourth and finally, another form of relationship exists between the two
480 types; where the lncRNA (>200 nucleotide) is capable of generating smaller (<22 nucleotide)
481 miRNAs such as the lncRNA H19 generating miR-675 [73]. GAS5 provides a perfect example for
482 such interactions. For instance, GAS5 acts as a molecular sponge for many different microRNAs,
483 including miR-21, miR-222, miR-196a, miR-205, miR-221 and miR-103. [16, 26, 74-77], all of
484 which are related to cancer. Then again, both miR-21 and miR-222 can negatively regulate *GAS5*
485 [27, 78]. Also, three of the snoRNAs produced by GAS5 (U44, U74 and U78) can give rise to

486 miRNAs [79], making GAS5 one of the lncRNAs generating miRNAs.

487 While functional validation has been yet required to prove the direct interaction between GAS5 and
488 miR-34a, it is highly plausible. This is due to the already verified interaction between miR-34a and
489 GAS1 (Growth arrest specific 1), another member of the *GAS* genes [42]. *GAS1* is a protein coding
490 gene that, similar to *GAS5*, exerts its tumor suppressor actions through arresting the cell cycle and
491 stimulating apoptosis [80]. Ma et al. measured the expression of miR-34a and the GAS1 protein in
492 papillary thyroid carcinoma; GAS1 was under-expressed, while miR-34a was over-expressed.
493 Further analysis revealed that miR-34a binds to the 3'UTR of GAS1 causing its silencing, which in
494 turn activates the *RET* oncogene [42]. Through the BLAST tool, we detected sequence homology
495 between the *GAS1* and the *GAS5* genes, further raising the possibility of interaction of miRNA-34a
496 with GAS5. Given that *GAS5* is down-regulated and *miR-34a* is up-regulated in our study,
497 tumorigenesis may be in such a case due to sponging of miR-34a by GAS5, where under-
498 expression of *GAS5* in the rapidly dividing cancer cells causes release of the inhibition of miR-34a
499 on its tumor suppressor targets, allowing for further tumor progression. Oppositely, the inverse
500 correlation between the two could also suggest that miR-34a inhibits GAS5, making its under-
501 expression a cause of cancer rather than a result, as in the case of the miR-34a -GAS1 interaction.

502 miR-34a expression levels in our study were not significant in the case of patients with HCC. *GAS5*
503 levels, however, were under-expressed in HCC patients. In addition, lower GAS5 levels were
504 associated with more numerous tumor foci. The same conclusions were reached by studies
505 conducted by Tu et al., Chang et al. and Hu et al. who found that *GAS5* was under-expressed in
506 HCC patients and predicted poor survival in those patients [15, 26, 81]. The latter study by Hu et al.
507 found that under-expression of *GAS5* in HCC cell lines releases its sponging effect on oncomiR-21,
508 which normally targets the two tumor suppressor genes *PDCD4* and *PTEN* [26]. On the contrary,
509 according to Tao et al., *GAS5* was a proto-oncogene in HCC where they found an indel
510 polymorphism in the promotor of *GAS5* that increased the risk of HCC in Chinese. In *vitro* analysis
511 showed that the deletion allele of the polymorphism altered methylation of the *GAS5* promoter and

512 was associated with higher levels of GAS5 in HCC cell lines Sk-hep-1, Bel-7404 and Huh7.
513 Further analysis provided evidence that the resulting over-expression of *GAS5* had an anti-apoptotic
514 effect in those cell lines [82]. This divergence observed by Tao et al. could be due to racial
515 differences. In other words, the allele causing *GAS5* over-expression might be more common in
516 their studied population. To further confirm this probability, we searched the 1000 genome project
517 phase 3 databases [83] for this indel polymorphism (positon 1:173868254-173868258 (AGGCA/-)).
518 We found that the frequency of the deletion allele was very high in Asians and Chinese in particular
519 (28-40%) as compared to other races (3-12%), showing that in other populations the effect of the
520 polymorphism on HCC and *GAS5* expression could be negligible.

521 In patients with GB, both GAS5 and miR-34a levels were significantly down-regulated. Zhang et
522 al. correlated the expression of five lncRNAs including GAS5 with GB, and found that higher
523 levels of GAS5 were associated with prolonged survival [84]. Zhao et al. found that *GAS5* was
524 under-expressed in glioma cell lines U87 and U251 and that its tumor suppressor role was through
525 targeting miR-222 [16]. The same author, in a more recent study, added another miRNA to the
526 targets of GAS5; miR-196a-5p, where *GAS5* under-expression in human glioma stem cells
527 enhanced tumor progression through inhibiting this miRNA [85]. Regarding the more controversial
528 *miR-34a*, studies on brain cancer, including GB and glioma agree on its role as a tumor suppressor
529 in this particular tissue; reviewed in [86], which fits in with its expression status in the present
530 study.

531 **Conclusions**

532 In this study, we show that *GAS5* is under-expressed in three types of tumors, in addition to being
533 associated with tumor prognosis in some types. Consequently, we believe that GAS5 could
534 potentially be used as a prognostic marker for cancer. Furthermore, in favor of this notion is the
535 predicted subcellular localization of GAS5 provided by our in *silico* analysis, which shows that
536 GAS5 is most significantly localized in the extracellular exosomes, supporting its existence in the
537 circulation and highlighting its putative role as a non-invasive biomarker which mirrors tissue

538 pathology. Furthermore, we suppose that miR-34a might be a potential target of GAS5, or *vice*
539 *versa*. However, we confirm that further studies are required to validate this interaction.

540 **Acknowledgements**

541 The authors thank the Center of Excellence in Molecular and Cellular Medicine and the Oncology
542 Diagnostic Unit, Suez Canal University, Ismailia, Egypt for providing the facilities for performing
543 the research work.

544 **Compliance with ethical standards**

545 **Conflicts of interest**

546 The authors declare that they have no competing interests.

547 **Funding**

548 None.

549 **References**

- 550 [1] WHO | Cancer [WWW Document], World Health Organization. Available from URL
551 <http://www.who.int/mediacentre/factsheets/fs297/en/> (accessed 9.2.18).
- 552 [2] Grandér D. How do mutated oncogenes and tumor suppressor genes cause cancer? *Med*
553 *Oncol.* 1998; 15:20–6. <https://doi.org/10.1007/BF02787340>
- 554 [3] ENCODE Project Consortium. An integrated encyclopedia of DNA elements in the human
555 genome. *Nature.* 2012;489:57–74. <https://doi.org/10.1038/nature11247>
- 556 [4] Paraskevopoulou MD, Hatzigeorgiou AG. Analyzing MiRNA–LncRNA Interactions, in:
557 Long Non-Coding RNAs, *Methods in Molecular Biology*. Humana Press, New York, NY,
558 2016; pp. 271–286. https://doi.org/10.1007/978-1-4939-3378-5_21
- 559 [5] Bartonicek N, Maag JLV, Dinger ME. Long noncoding RNAs in cancer: mechanisms of
560 action and technological advancements. *Mol Cancer.* 2016; 15:43.
561 <https://doi.org/10.1186/s12943-016-0530-6>
- 562 [6] Leva GD, Garofalo M, Croce CM. MicroRNAs in Cancer. *Annu Rev Pathol Mech Dis.*
563 2014; 9:287–314. <https://doi.org/10.1146/annurev-pathol-012513-104715>

- 564 [7] Mannoor K, Liao J, Jiang F. Small nucleolar RNAs in cancer. *Biochim Biophys Acta*. 2012;
565 1826. <https://doi.org/10.1016/j.bbcan.2012.03.005>
- 566 [8] Ng KW, Anderson C, Marshall EA, Minatel BC, Enfield KSS, Saprunoff HL, et al. Piwi-
567 interacting RNAs in cancer: emerging functions and clinical utility. *Mol Cancer*. 2016; 15:5.
568 <https://doi.org/10.1186/s12943-016-0491-9>
- 569 [9] Lo P-K, Wolfson B, Zhou X, Duru N, Gernapudi R, Zhou Q. Noncoding RNAs in breast
570 cancer. *Brief Funct Genomics*. 2016; 15: 200–21. <https://doi.org/10.1093/bfpg/elv055>
- 571 [10] Raho G, Barone V, Rossi D, Philipson L, Sorrentino V. The gas 5 gene shows four
572 alternative splicing patterns without coding for a protein. *Gene*. 2000; 256:13–7.
573 [https://doi.org/10.1016/S0378-1119\(00\)00363-2](https://doi.org/10.1016/S0378-1119(00)00363-2)
- 574 [11] Smith CM, Steitz JA. Classification of gas5 as a Multi-Small-Nucleolar-RNA (snoRNA)
575 Host Gene and a Member of the 5'-Terminal Oligopyrimidine Gene Family Reveals
576 Common Features of snoRNA Host Genes. *Mol Cell Biol*. 1998;18:6897-909.
- 577 [12] Maden BE, Hughes JM. Eukaryotic ribosomal RNA: the recent excitement in the
578 nucleotide modification problem. *Chromosoma*. 1997; 105:391–400.
- 579 [13] Schneider C, King RM, Philipson L. Genes specifically expressed at growth arrest of
580 mammalian cells. *Cell*. 1988; 54:787–93.
- 581 [14] Coccia EM, Cicala C, Charlesworth A, Ciccarelli C, Rossi G B, Philipson L, et al.
582 Regulation and expression of a growth arrest-specific gene (gas5) during growth,
583 differentiation, and development. *Molecular and Cellular Biology*. 1992; 12:3514-21.
- 584 [15] Chang L, Li C, Lan T, Long Wu, Yufeng Yuan, Quanyan Liuet, al. Decreased expression
585 of long non-coding RNA GAS5 indicates a poor prognosis and promotes cell proliferation
586 and invasion in hepatocellular carcinoma by regulating vimentin. *Mol Med Rep*. 2016;
587 13:1541-50. <https://doi.org/10.3892/mmr.2015.4716>
- 588 [16] Xihe Zhao, Ping Wang, Jing Liu, Jian Zheng, Yunhui Liu, Jiajia Chen et al. Gas5 Exerts
589 Tumor-suppressive Functions in Human Glioma Cells by Targeting miR-222. *Mol Ther*.

- 590 23:1899–911. <https://doi.org/10.1038/mt.2015.170>
- 591 [17] Wenjun Liang, Tangfeng Lv, Xuefei Shi, Hongbing Liu, Qingqing Zhu, Junli Zeng, et al.
592 Circulating long noncoding RNA GAS5 is a novel biomarker for the diagnosis of nonsmall
593 cell lung cancer. *Medicine (Baltimore)*. 2016; 95:e4608.
594 <https://doi.org/10.1097/MD.0000000000004608>
- 595 [18] Cao Q, Wang N, Qi J, Gu Z, Shen H. Long non-coding RNA-GAS5 acts as a tumor
596 suppressor in bladder transitional cell carcinoma via regulation of chemokine (C-C motif)
597 ligand 1 expression. *Mol Med Rep*. 2016; 13:27–34. <https://doi.org/10.3892/mmr.2015.4503>
- 598 [19] Yacqub-Usman K, Pickard MR, Williams GT. Reciprocal regulation of GAS5 lncRNA
599 levels and mTOR inhibitor action in prostate cancer cells. *The Prostate* 2015; 75:693–705.
600 <https://doi.org/10.1002/pros.22952>
- 601 [20] Pickard MR, Williams GT 2014. Regulation of apoptosis by long non-coding RNA GAS5
602 in breast cancer cells: implications for chemotherapy. *Breast Cancer Res Treat*. 2014;
603 145:359–70. <https://doi.org/10.1007/s10549-014-2974-y>
- 604 [21] Guo C, Song W-Q, Sun P, Jin L, Dai H-Y. LncRNA-GAS5 induces PTEN expression
605 through inhibiting miR-103 in endometrial cancer cells. *J. Biomed. Sci*. 2015; 22:100.
606 <https://doi.org/10.1186/s12929-015-0213-4>
- 607 [22] Lu X, Fang Y, Wang Z, Xie J, Zhan Q, Deng X, et al. Downregulation of gas5 increases
608 pancreatic cancer cell proliferation by regulating CDK6. *Cell Tissue Res*. 2013; 354:891–6.
609 <https://doi.org/10.1007/s00441-013-1711-x>
- 610 [23] Yin D, He X, Zhang E, Kong R, De W, Zhang Z. Long noncoding RNA GAS5 affects cell
611 proliferation and predicts a poor prognosis in patients with colorectal cancer. *Med Oncol*
612 Northwood Lond Engl. 2014; 31:253. <https://doi.org/10.1007/s12032-014-0253-8>
- 613 [24] Qiao H-P, Gao W-S, Huo J-X, Yang Z-S. Long Non-coding RNA GAS5 Functions as a
614 Tumor Suppressor in Renal Cell Carcinoma. *Asian Pac J Cancer Prev*. 2013; 14: 1077–82.
615 <https://doi.org/10.7314/APJCP.2013.14.2.1077>

- 616 [25] Nakamura Y, Takahashi N, Kakegawa E, Yoshida K, Ito Y, Kayano H, et al. The GAS5
617 (growth arrest-specific transcript 5) gene fuses to BCL6 as a result of t(1;3) (q25;q27) in a
618 patient with B-cell lymphoma. *Cancer Genet. Cytogenet.* 2008; 182:144–9.
619 <https://doi.org/10.1016/j.cancergencyto.2008.01.013>
- 620 [26] Hu L, Ye H, Huang G, Luo F, Liu Y, Liu Y, et al. Long noncoding RNA GAS5
621 suppresses the migration and invasion of hepatocellular carcinoma cells via miR-21.
622 *Tumour Biol.* 2016; 37:2691–702. <https://doi.org/10.1007/s13277-015-4111-x>
- 623 [27] Zhang Z, Zhu Z, Watabe K, Zhang X, Bai C, Xu M, et al. Negative regulation of lncRNA
624 GAS5 by miR-21. *Cell Death Differ.* 2013; 20:1558–68.
625 <https://doi.org/10.1038/cdd.2013.110>
- 626 [28] He L, He X, Lim LP, de Stanchina E, Xuan Z, Liang Y, et al. A microRNA component of
627 the p53 tumour suppressor network. *Nature.* 2007; 447:1130–4.
628 <https://doi.org/10.1038/nature05939>
- 629 [29] Lodygin D, Tarasov V, Epanchintsev A, Berking C, Knyazeva T, Körner H, et al.
630 Inactivation of miR-34a by aberrant CpG methylation in multiple types of cancer. *Cell*
631 *Cycle.* 2008; 7:2591–600. <https://doi.org/10.4161/cc.7.16.6533>
- 632 [30] Welch C, Chen Y, Stallings RL. MicroRNA-34a functions as a potential tumor suppressor
633 by inducing apoptosis in neuroblastoma cells. *Oncogene.* 2007; 26:5017–22.
634 <https://doi.org/10.1038/sj.onc.1210293>
- 635 [31] Chim CS, Wong KY, Qi Y, Loong F, Lam WL, Wong LG, et al. Epigenetic inactivation
636 of the miR-34a in hematological malignancies. *Carcinogenesis.* 2010; 31: 745–50.
637 <https://doi.org/10.1093/carcin/bgq033>
- 638 [32] Ji Q, Hao X, Zhang M, Tang W, Yang M, Li L, et al. MicroRNA miR-34 inhibits human
639 pancreatic cancer tumor-initiating cells. *PloS One.* 2009; 4:e6816.
640 <https://doi.org/10.1371/journal.pone.0006816>
- 641 [33] Li N, Fu H, Tie Y, Hu Z, Kong W, Wu Y, et al. miR-34a inhibits migration and invasion

- 642 by down-regulation of c-Met expression in human hepatocellular carcinoma cells. *Cancer*
643 *Lett.* 2009; 275:44–53. <https://doi.org/10.1016/j.canlet.2008.09.035>
- 644 [34] Shehata RH, Abdelmoneim SS, Osman OA, Hasanain AF, Osama A, Abdelmoneim SS, et
645 al. Deregulation of miR-34a and Its Chaperon Hsp70 in Hepatitis C virus-Induced Liver
646 Cirrhosis and Hepatocellular Carcinoma Patients. *Asian Pacific Journal of Cancer*
647 *Prevention. APJCP.* 2017;18(9):2395-2401. doi:10.22034/APJCP.2017.18.9.2395
- 648 [35] Li Y, Guessous F, Zhang Y, Dipierro C, Kefas B, Johnson E, et al. MicroRNA-34a
649 inhibits glioblastoma growth by targeting multiple oncogenes. *Cancer Res.* 2009; 69: 7569–
650 76. <https://doi.org/10.1158/0008-5472.CAN-09-0529>
- 651 [36] Toraih EA, Aly NM, Abdallah HY, Al-Qahtani SA, Shaalan AA, Hussein MH, et al.
652 MicroRNA-target cross-talks: Key players in glioblastoma multiforme. *Tumour Biol.*
653 2017;39(11):1010428317726842. <https://doi.org/10.1177/1010428317726842>
- 654 [37] Kato M1, Paranjape T, Müller RU, Nallur S, Gillespie E, Keane K, et al. The mir-34
655 microRNA is required for the DNA damage response in vivo in *C. elegans* and in vitro in
656 human breast cancer cells. *Oncogene.* 2009; 28:2419–24.
657 <https://doi.org/10.1038/onc.2009.106>
- 658 [38] Wiggins JF, Ruffino L, Kelnar K, Omotola M, Patrawala L, Brown D, et al. Development
659 of a lung cancer therapeutic based on the tumor suppressor microRNA-34. *Cancer Res.*
660 2010; 70:5923–30. <https://doi.org/10.1158/0008-5472.CAN-10-0655>
- 661 [39] Tazawa H, Tsuchiya N, Izumiya M, Nakagama H. Tumor-suppressive miR-34a induces
662 senescence-like growth arrest through modulation of the E2F pathway in human colon
663 cancer cells. *Proc Natl Acad Sci USA.* 2007; 104:15472–7.
664 <https://doi.org/10.1073/pnas.0707351104>
- 665 [40] Liu H, Brannon AR, Reddy AR, Alexe G, Seiler MW, Arreola A, et al. Identifying mRNA
666 targets of microRNA dysregulated in cancer: with application to clear cell Renal Cell
667 Carcinoma. *BMC Syst Biol.* 2010; 4:51. <https://doi.org/10.1186/1752-0509-4-51>

- 668 [41] Toraih EA, Ibrahiem AT, Fawzy MS, Hussein MH, Al-Qahtani SAM, Shaalan AAM.
669 MicroRNA-34a: A Key Regulator in the Hallmarks of Renal Cell Carcinoma. *Oxid Med*
670 *Cell Longev.* 2017; 2017:3269379. <https://doi.org/10.1155/2017/3269379>
- 671 [42] Ma Y, Qin H, Cui Y. MiR-34a targets GAS1 to promote cell proliferation and inhibit
672 apoptosis in papillary thyroid carcinoma via PI3K/Akt/Bad pathway. *Biochem Biophys Res*
673 *Commun.* 2013; 441:958–63. <https://doi.org/10.1016/j.bbrc.2013.11.01043>. Tazawa et al.,
674 2007
- 675 [43] Marsh EE1, Lin Z, Yin P, Milad M, Chakravarti D, Bulun SE. Differential expression of
676 microRNA species in human uterine leiomyoma versus normal myometrium. *Fertil Steril.*
677 2008; 89:1771–6. <https://doi.org/10.1016/j.fertnstert.2007.05.074>
- 678 [44] Llovet JM, Fuster J, Bruix J. Barcelona-Clinic Liver Cancer Group. The Barcelona
679 approach: diagnosis, staging, and treatment of hepatocellular carcinoma. *Liver Transpl.*
680 2004; 10:S115-20. doi: 10.1002/lt.20034
- 681 [45] Toraih EA, Fawzy MS, El-Falouji AI, Elham O Hamed, Nader A Nemr, Mohammad H
682 Hussein, et al. Stemness-Related Transcriptional Factors and Homing Gene Expression
683 Profiles in Hepatic Differentiation and Cancer. *Mol Med.* 2016; 22:653-63.
684 <https://doi.org/10.2119/molmed.2016.00096>
- 685 [46] Toraih EA, Fawzy MS, Mohammed EA, Hussein MH, El-Labban MM. MicroRNA-196a2
686 Biomarker and Targetome Network Analysis in Solid Tumors. *Mol Diagn Ther.* 2016;
687 20:559-77. <https://doi.org/10.1007/s40291-016-0223-2>
- 688 [47] Bustin SA, Benes V, Garson JA, Hellemans J, Huggett J, Kubista M, et al. The MIQE
689 guidelines: minimum information for publication of quantitative real-time PCR experiments.
690 *Clin Chem.* 2009; 55:611–22. <https://doi.org/10.1373/clinchem.2008.112797>
- 691 [48] Toraih EA, Mohammed EA, Farrag S, Ramsis N, Hosny S. Pilot Study of Serum
692 MicroRNA-21 as a Diagnostic and Prognostic Biomarker in Egyptian Breast Cancer
693 Patients. *Mol Diagn Ther.* 2015; 19:179-90. <https://doi.org/10.1007/s40291-015-0143-6>.

- 694 [49] Valente V, Teixeira SA, Neder L, Okamoto OK, Oba-Shinjo SM, Marie SK, et al.
695 Selection of suitable housekeeping genes for expression analysis in glioblastoma using
696 quantitative RT-PCR. *Ann Neurosci*. 2014; 21(2):62-3.
697 <https://doi.org/10.5214/ans.0972.7531.210207>
- 698 [50] Aithal MGS, Rajeswari N. Validation of Housekeeping Genes for Gene Expression
699 Analysis in Glioblastoma Using Quantitative Real-Time Polymerase Chain Reaction. *Brain*
700 *Tumor Res Treat*. 2015; 3:24-29. <https://doi.org/10.14791/btrt.2015.3.1.24>.
- 701 [51] Livak KJ, Schmittgen TD. Analysis of relative gene expression data using real-time
702 quantitative PCR and the 2⁻(-Delta Delta C (T)) Method. *Methods*. 2001, 25:402–8.
703 <https://doi.org/10.1006/meth.2001.1262>
- 704 [52] McCune B, Mefford MJ. PC-ORD. Multivariate Analysis of Ecological Data. Version 6.
705 MjM Software, Gleneden Beach, Oregon, USA, 2011.
- 706 [53] Yamashita R, Suzuki Y, Takeuchi N, Wakaguri H, Ueda T, Sugano S, et al.
707 Comprehensive detection of human terminal oligo-pyrimidine (TOP) genes and analysis of
708 their characteristics. *Nucleic Acids Res*. 2008; 36:3707-15.
709 <https://doi.org/10.1093/nar/gkn248>
- 710 [54] Cheng T, Wang L, Li Y, Huang C, Zeng L, Yang J. Differential microRNA expression in
711 renal cell carcinoma. *Oncol Lett*. 2013; 6:769–76. <https://doi.org/10.3892/ol.2013.1460>
- 712 [55] Munari E, Marchionni L, Chitre A, Hayashi M, Martignoni G, Brunelli M, et al. Clear cell
713 papillary renal cell carcinoma: micro-RNA expression profiling and comparison with clear
714 cell renal cell carcinoma and papillary renal cell carcinoma. *Hum Pathol*. 2014; 45:1130–8.
715 <https://doi.org/10.1016/j.humpath.2014.01.013>
- 716 [56] Fritz HK, Gustafsson A, Ljungberg B, Ceder Y, Axelson H, Dahlbäck B. The Axl-
717 Regulating Tumor Suppressor miR-34a Is Increased in ccRCC but Does Not Correlate with
718 Axl mRNA or Axl Protein Levels. *PloS One*. 2015; 10:e0135991.
719 <https://doi.org/10.1371/journal.pone.0135991>

- 720 [57] Bhatt K, Zhou L, Mi QS, Huang S, She JX, Dong Z. MicroRNA-34a is induced via p53
721 during cisplatin nephrotoxicity and contributes to cell survival. *Mol Med.* 2010; 16:409–16.
722 <https://doi.org/10.2119/molmed.2010.00002>
- 723 [58] Yadav S, Khandelwal M, Seth A, Saini AK, Dogra PN, Sharma A. Serum microRNA
724 Expression Profiling: Potential Diagnostic Implications of a Panel of Serum microRNAs for
725 Clear Cell Renal Cell Cancer. *Urology.* 2017; 104:64–9.
726 <https://doi.org/10.1016/j.urology.2017.03.013>
- 727 [59] Zhang EB, Kong R, Yin DD, You LH, Sun M, Han L, et al. Long noncoding RNA
728 ANRIL indicates a poor prognosis of gastric cancer and promotes tumor growth by
729 epigenetically silencing of miR-99a/miR-449a. *Oncotarget.* 5:2276–92.
730 <https://doi.org/10.18632/oncotarget.1902>
- 731 [60] Weng W, Wang M, Xie S, Long Y, Li F, Sun F, et al. YY1-C/EBP α -miR34a regulatory
732 circuitry is involved in renal cell carcinoma progression. *Oncol Rep.* 2014; 31:1921–7.
733 <https://doi.org/10.3892/or.2014.3005>
- 734 [61] Yu G, Li H, Wang J, Gumireddy K, Li A, Yao W, et al. miRNA-34a Suppresses Cell
735 Proliferation and Metastasis by Targeting CD44 in Human Renal Carcinoma Cells. *J Urol.*
736 2014; 192:1229–37. <https://doi.org/10.1016/j.juro.2014.05.094>
- 737 [62] Yamamura S, Saini S, Majid S, Hirata H, Ueno K, Chang I, et al. MicroRNA-34a
738 suppresses malignant transformation by targeting c-Myc transcriptional complexes in
739 human renal cell carcinoma. *Carcinogenesis.* 2012; 33:294–300.
740 <https://doi.org/10.1093/carcin/bgr286>
- 741 [63] Liu F, Chen N, Gong Y, Xiao R, Wang W, Pan Z. The long non-coding RNA NEAT1
742 enhances epithelial-to-mesenchymal transition and chemoresistance via the miR-34a/c-Met
743 axis in renal cell carcinoma. *Oncotarget.* 2017; 8:62927–38.
744 <https://doi.org/10.18632/oncotarget.17757>
- 745 [64] Bai XY, Ma Y, Ding R, Fu B, Shi S, Chen XM. miR-335 and miR-34a Promote Renal

- 746 Senescence by Suppressing Mitochondrial Antioxidative Enzymes. *J Am Soc Nephrol.*
747 2011; 22:1252–61. <https://doi.org/10.1681/ASN.2010040367>
- 748 [65] Collado M, Blasco MA, Serrano M. Cellular Senescence in Cancer and Aging. *Cell.* 2007;
749 130:223–33. <https://doi.org/10.1016/j.cell.2007.07.003>
- 750 [66] Zhou Y, Xiong M, Niu J, Sun Q, Su W, Zen K, et al. Secreted fibroblast-derived miR-34a
751 induces tubular cell apoptosis in fibrotic kidney. *J Cell Sci.* 2014; 127:4494–506.
752 <https://doi.org/10.1242/jcs.155523>
- 753 [67] Borrell B. How accurate are cancer cell lines? *Nature.* 2010; 463:858.
754 <https://doi.org/10.1038/463858a>
- 755 [68] Clark MJ, Homer N, O'Connor BD, Chen Z, Eskin A, Lee H, et al. U87MG Decoded: The
756 Genomic Sequence of a Cytogenetically Aberrant Human Cancer Cell Line. *PLoS Genet.*
757 2010; 6:e1000832. <https://doi.org/10.1371/journal.pgen.1000832>
- 758 [69] Yoon JH, Abdelmohsen K, Srikantan S, Yang X, Martindale JL, De S, et al. LincRNA-
759 p21 suppresses target mRNA translation. *Mol Cell.* 2012; 47:648–55.
760 <https://doi.org/10.1016/j.molcel.2012.06.027>
- 761 [70] Wang Y, Xu Z, Jiang J, Xu C, Kang J, Xiao L, et al. Endogenous miRNA Sponge
762 lincRNA-RoR Regulates Oct4, Nanog, and Sox2 in Human Embryonic Stem Cell Self-
763 Renewal. *Dev Cell.* 2013; 25:69–80. <https://doi.org/10.1016/j.devcel.2013.03.002>
- 764 [71] Leucci E, Patella F, Waage J, Holmstrøm K, Lindow M, Porse B, et al. microRNA-9
765 targets the long non-coding RNA MALAT1 for degradation in the nucleus. *Sci Rep.* 2013;
766 3:2535. <https://doi.org/10.1038/srep02535>
- 767 [72] Faghihi MA, Zhang M, Huang J, Modarresi F, Van der Brug MP, Nalls MA, et al.
768 Evidence for natural antisense transcript-mediated inhibition of microRNA function.
769 *Genome Biol.* 2010; 11: R56. <https://doi.org/10.1186/gb-2010-11-5-r56>
- 770 [73] Keniry A1, Oxley D, Monnier P, Kyba M, Dandolo L, Smits G, et al. The H19 lincRNA is
771 a developmental reservoir of miR-675 that suppresses growth and Igf1r. *Nat Cell Biol.*

- 772 2012; 14:659–65. <https://doi.org/10.1038/ncb2521>
- 773 [74] Guo C, Song WQ, Sun P, Jin L, Dai HY. LncRNA-GAS5 induces PTEN expression
774 through inhibiting miR-103 in endometrial cancer cells. *J Biomed Sci.* 2015; 22:100.
775 <https://doi.org/10.1186/s12929-015-0213-4>
- 776 [75] Xue D, Zhou C, Lu H, Xu R, Xu X, He X. LncRNA GAS5 inhibits proliferation and
777 progression of prostate cancer by targeting miR-103 through AKT/mTOR signaling
778 pathway. *Tumor Biol.* 2016; 37:16187–97. <https://doi.org/10.1007/s13277-016-5429-8>
- 779 [76] Yang W, Hong L, Xu X, Wang Q, Huang J, Jiang L. LncRNA GAS5 suppresses the
780 tumorigenesis of cervical cancer by downregulating miR-196a and miR-205. *Tumour Biol.*
781 2017; 39:1010428317711315. <https://doi.org/10.1177/1010428317711315>
- 782 [77] Ye K, Wang S, Zhang H, Han H, Ma B, Nan W. Long Noncoding RNA GAS5 Suppresses
783 Cell Growth and Epithelial-Mesenchymal Transition in Osteosarcoma by Regulating the
784 miR-221/ARHI Pathway. *J Cell Biochem.* 2017; 118:4772-81.
785 <https://doi.org/10.1002/jcb.26145>
- 786 [78] Yu F, Zheng J, Mao Y, Dong P, Lu Z, Li G, et al. Long Non-coding RNA Growth Arrest-
787 specific Transcript 5 (GAS5) Inhibits Liver Fibrogenesis through a Mechanism of
788 Competing Endogenous RNA. *J Biol Chem.* 2015; 290:28286–98.
789 <https://doi.org/10.1074/jbc.M115.683813>
- 790 [79] Brameier M, Herwig A, Reinhardt R, Walter L, Gruber J. Human box C/D snoRNAs with
791 miRNA like functions: expanding the range of regulatory RNAs. *Nucleic Acids Res.* 2011;
792 39:675–86. <https://doi.org/10.1093/nar/gkq776>
- 793 [80] Domínguez-Monzón G, Benítez JA, Vergara P, Lorenzana R, Segovia J. Gas1 inhibits cell
794 proliferation and induces apoptosis of human primary gliomas in the absence of Shh. *Int J*
795 *Dev Neurosci.* 2009; 27:305–13. <https://doi.org/10.1016/j.ijdevneu.2009.03.009>
- 796 [81] Tu ZQ, Li RJ, Mei JZ, Li XH. Down-regulation of long non-coding RNA GAS5 is
797 associated with the prognosis of hepatocellular carcinoma. *Int. J Clin Exp Pathol.* 2014;

- 798 7:4303–9.
- 799 [82] Tao R, Hu S, Wang S, Zhou X, Zhang Q, Wang C, et al. Association between indel
800 polymorphism in the promoter region of lncRNA GAS5 and the risk of hepatocellular
801 carcinoma. *Carcinogenesis*. 2015; 36:1136–43. <https://doi.org/10.1093/carcin/bgv099>
- 802 [83] The 1000 Genomes Project Consortium. A global reference for human genetic variation.
803 *Nature*. 2015; 526:68–74. <https://doi.org/10.1038/nature15393>
- 804 [84] Zhang XQ, Sun S, Lam KF, Kiang KM, Pu JK, Ho AS, et al. A long non-coding RNA
805 signature in glioblastoma multiforme predicts survival. *Neurobiol Dis*. 2013; 58:123–31.
806 <https://doi.org/10.1016/j.nbd.2013.05.011>
- 807 [85] Zhao X, Liu Y, Zheng J, Liu X, Chen J, Liu L, et al. GAS5 suppresses malignancy of
808 human glioma stem cells via a miR-196a-5p/FOXO1 feedback loop. *Biochim Biophys Acta*.
809 2017; 1864:1605–17. <https://doi.org/10.1016/j.bbamcr.2017.06.020>
- 810 [86] Møller HG, Rasmussen AP, Andersen HH, Johnsen KB, Henriksen M, Duroux M. A
811 Systematic Review of MicroRNA in Glioblastoma Multiforme: Micro-modulators in the
812 Mesenchymal Mode of Migration and Invasion. *Mol Neurobiol*. 2013; 47:131–44.
813 <https://doi.org/10.1007/s12035-012-8349-7>

814

815 **Supporting Information**

816 **S1 Table: GAS5 alternative splicing transcripts.**

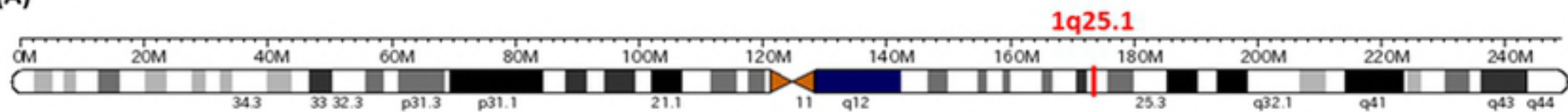
817 **S2 Table: GAS5 common variants.**

818 **S3 Table: LncRNA GAS5-microRNA interaction.**

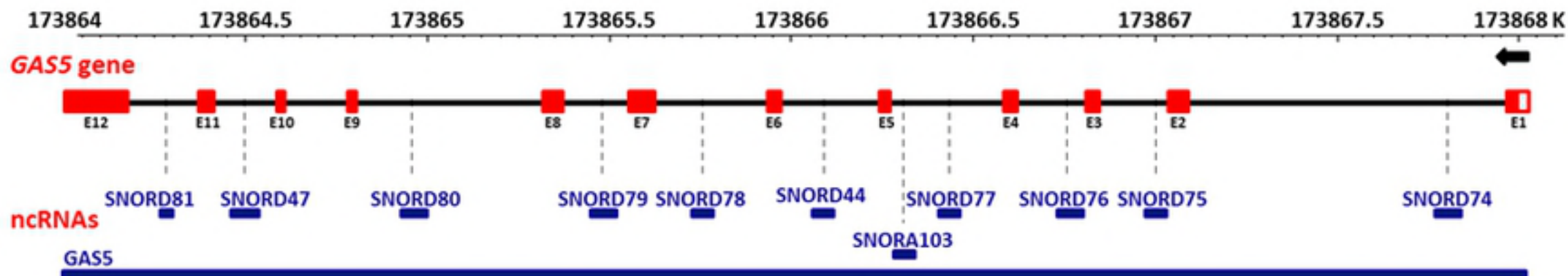
819 **S4 Table: Complementarity between GAS5 transcripts and miR-34a-5p.**

820 **S5 Table: hsa-miR-34a pathways.**

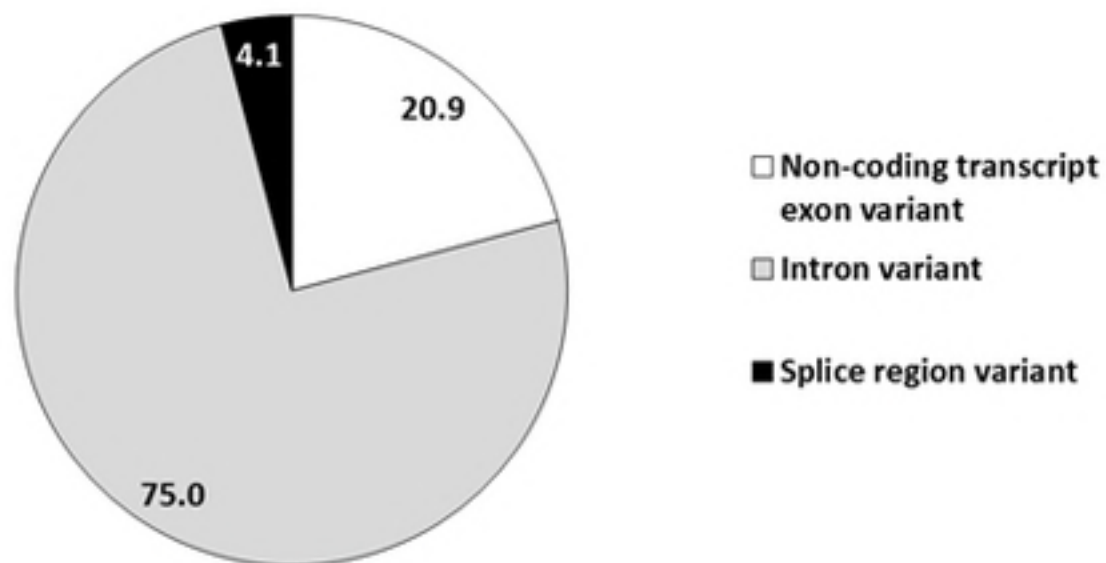
(A)



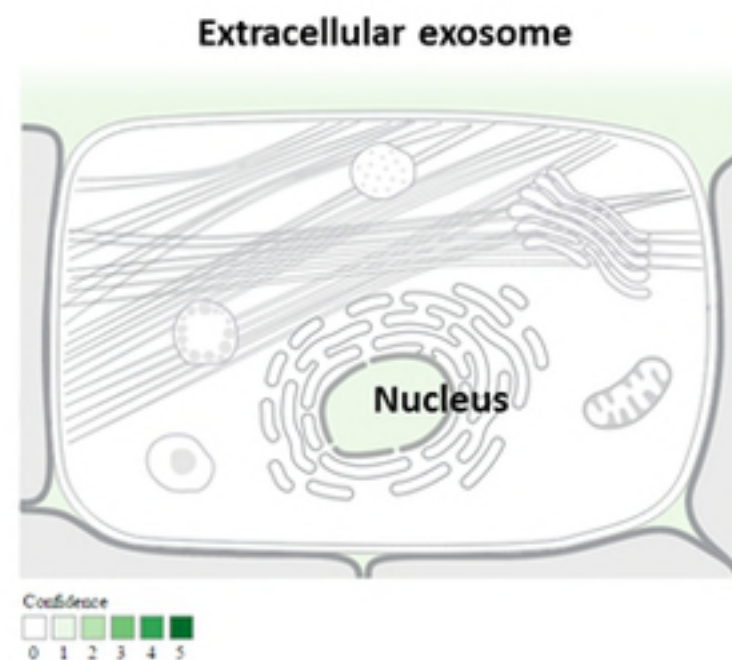
(B)



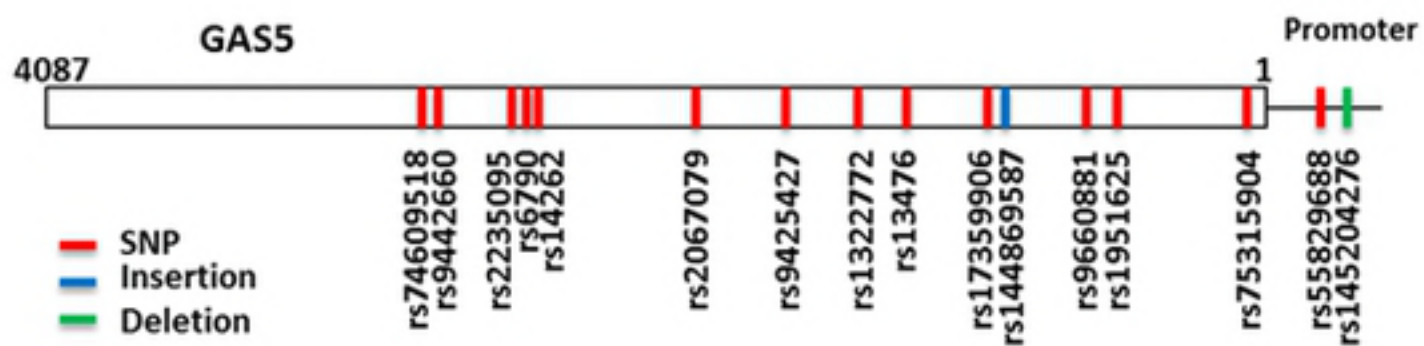
(C)



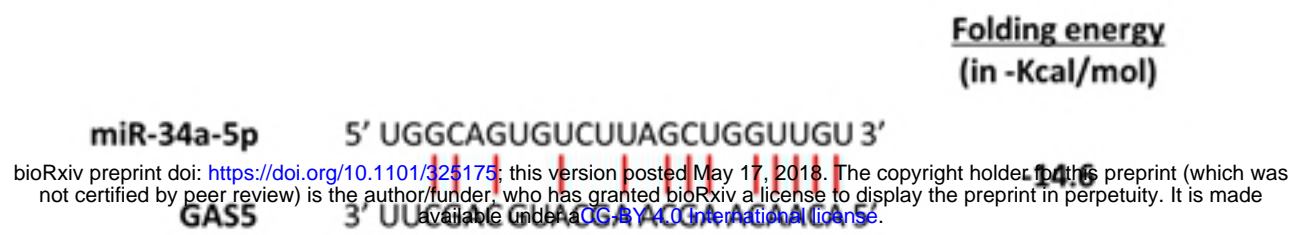
(D)



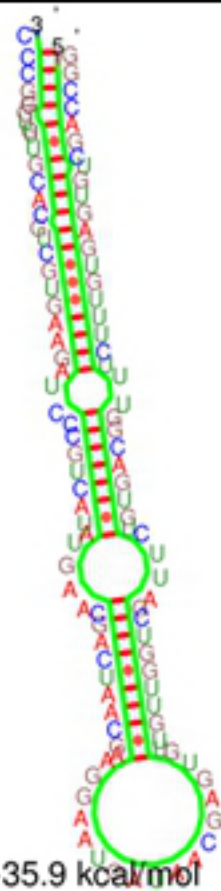
(E)



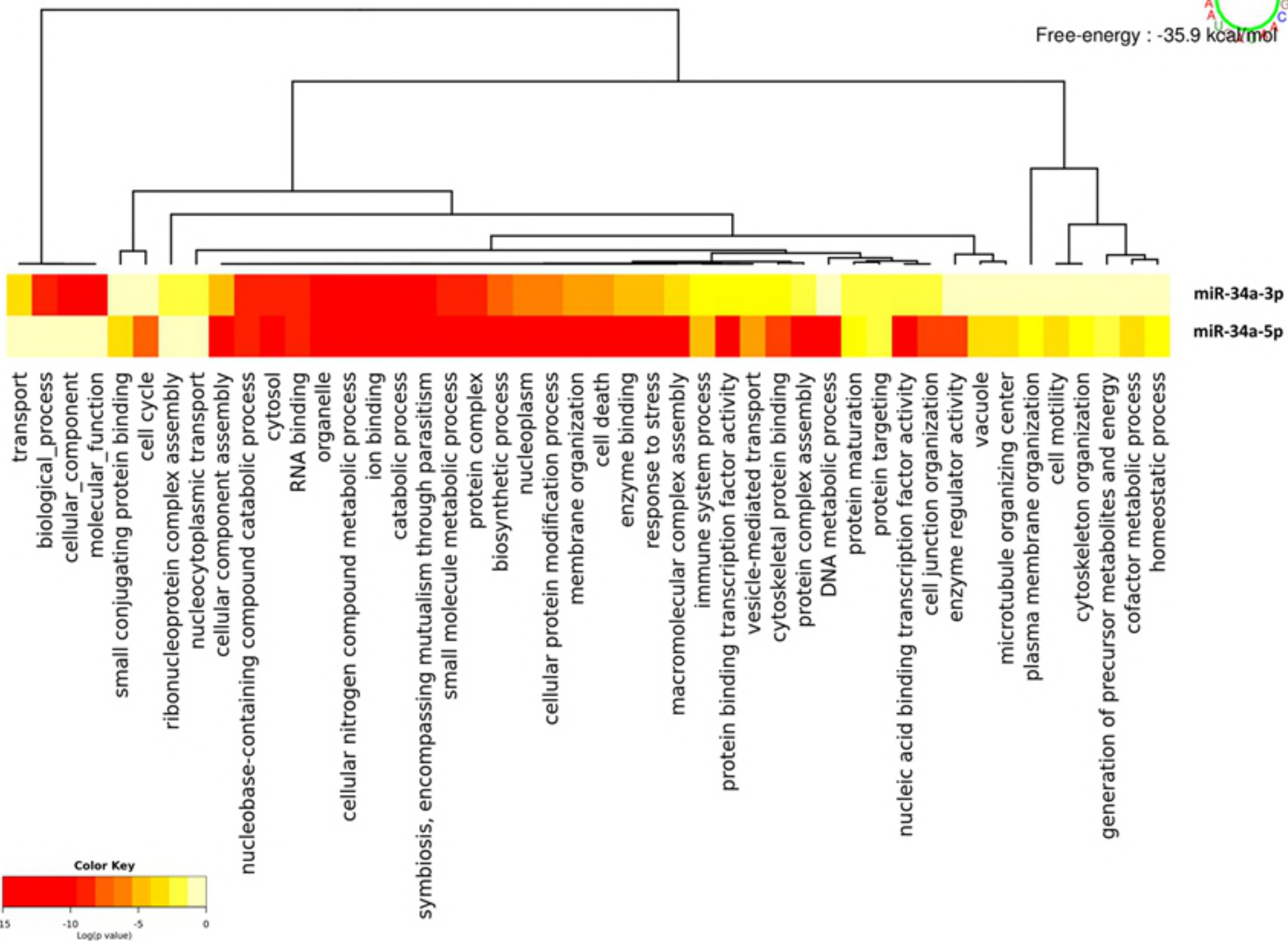
(A)



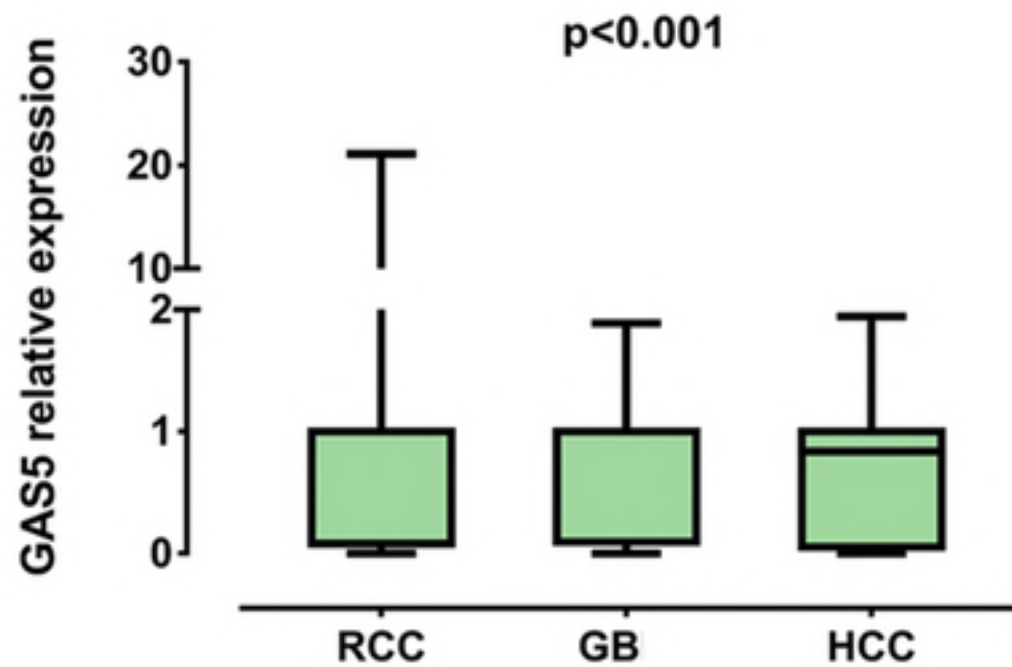
(B)



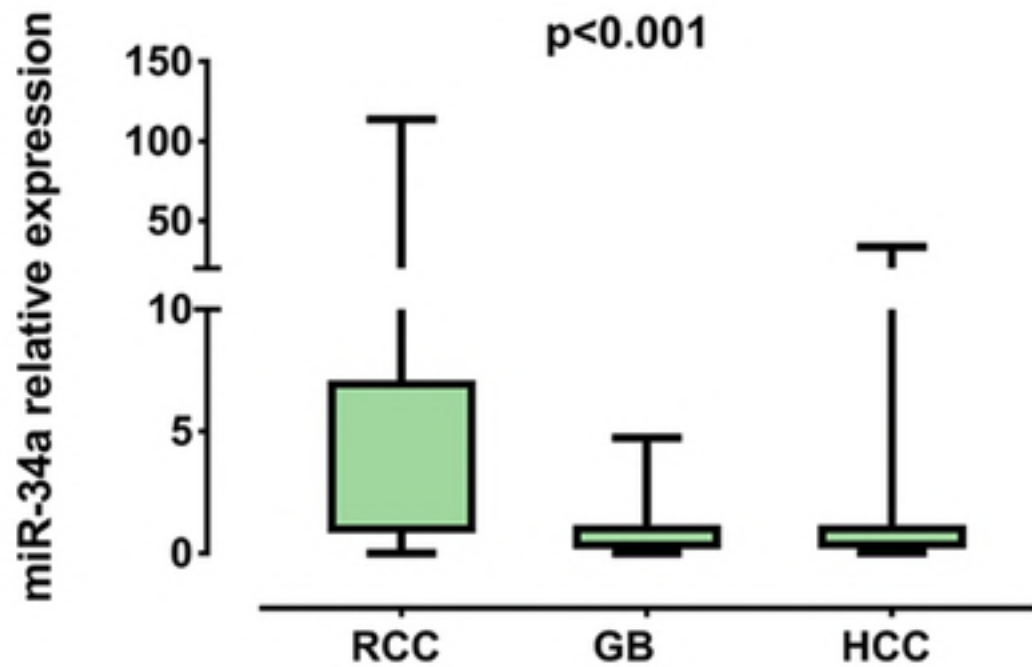
(C)

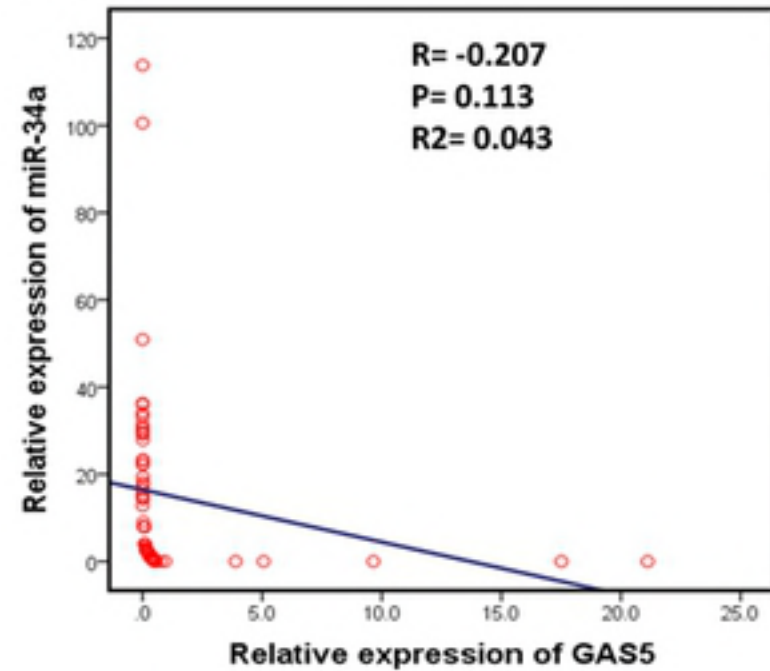
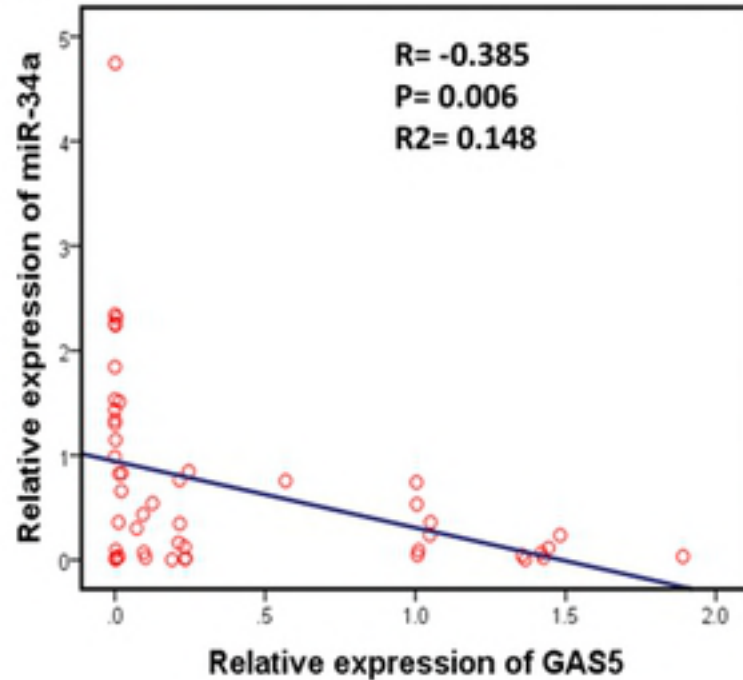
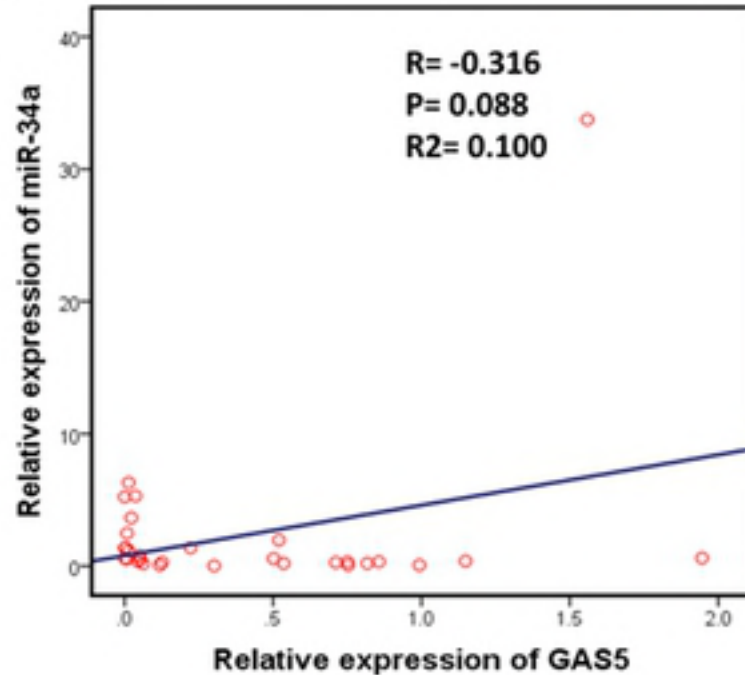


(A)



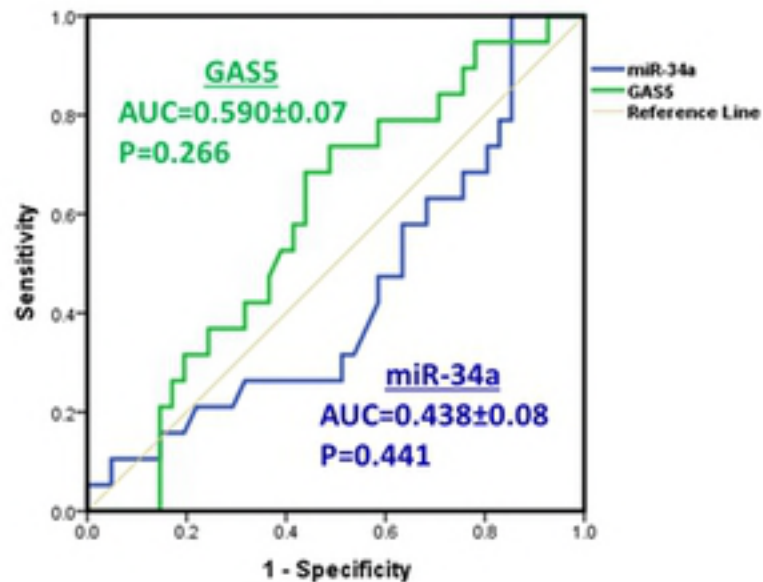
(B)



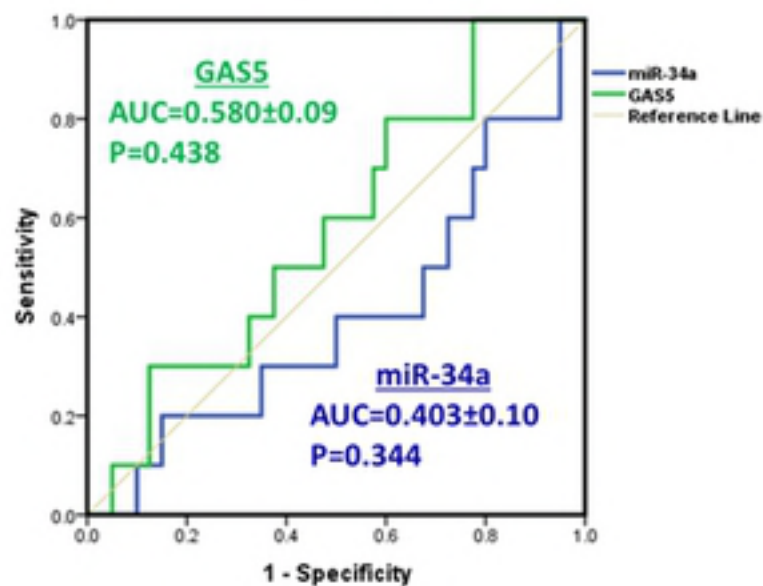
(A) RCC**(B) GB****(C) HCC**

(A) RCC

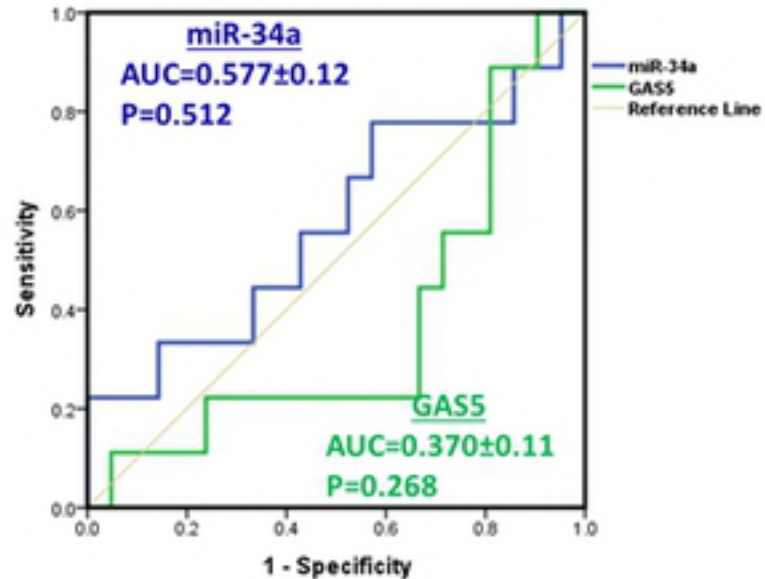
Overall survival in RCC

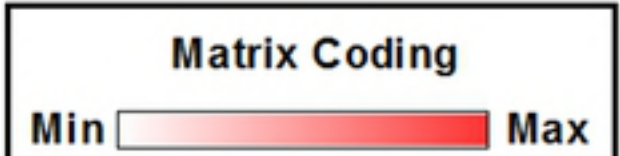
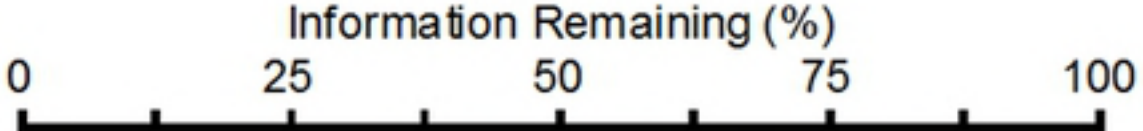
**(B) GB**

Overall survival in GB

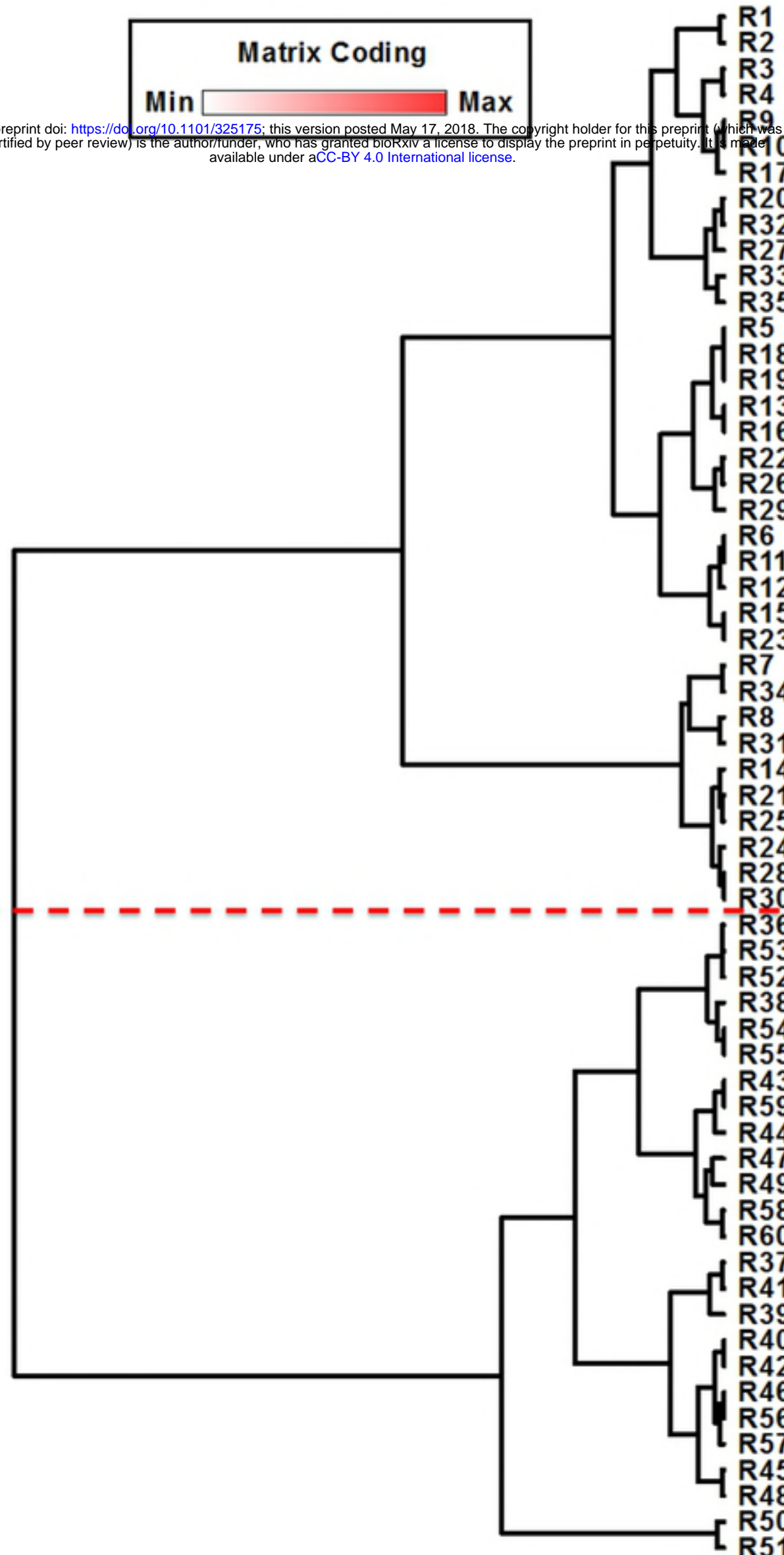
**(C) HCC**

CTP class in HCC



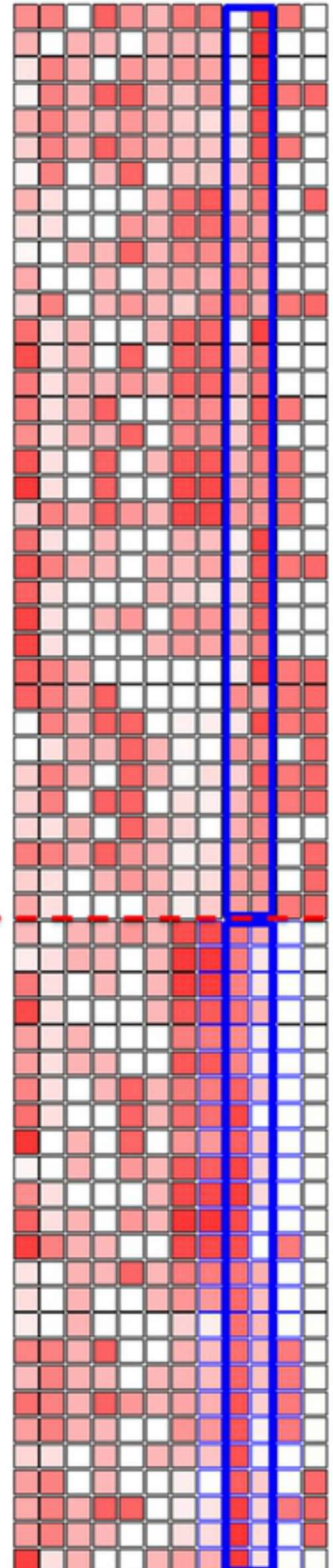


bioRxiv preprint doi: <https://doi.org/10.1101/325175>; this version posted May 17, 2018. The copyright holder for this preprint (which was not certified by peer review) is the author/funder, who has granted bioRxiv a license to display the preprint in perpetuity. It is made available under aCC-BY 4.0 International license.



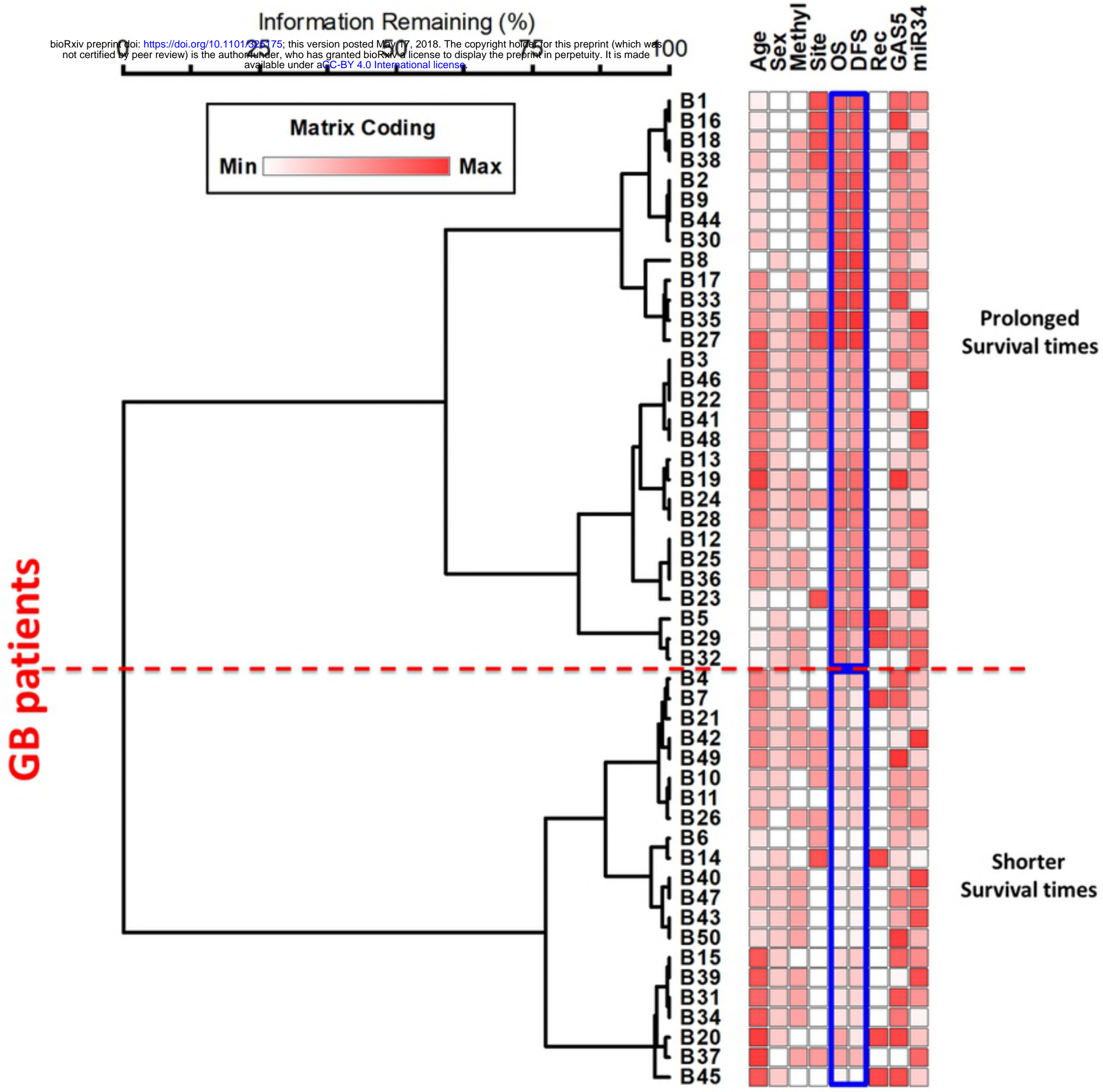
RCC patients

Age
Grade
Side
T
HPD
Gender
PFS
OS
miR34a
GAS5
LN
recurr



Low miR-34a
High GAS5

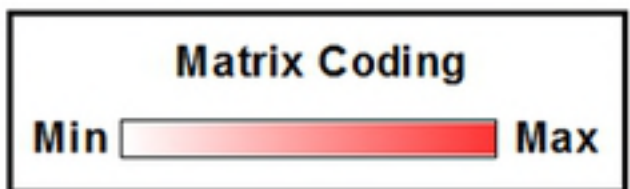
High miR-34a
Low GAS5



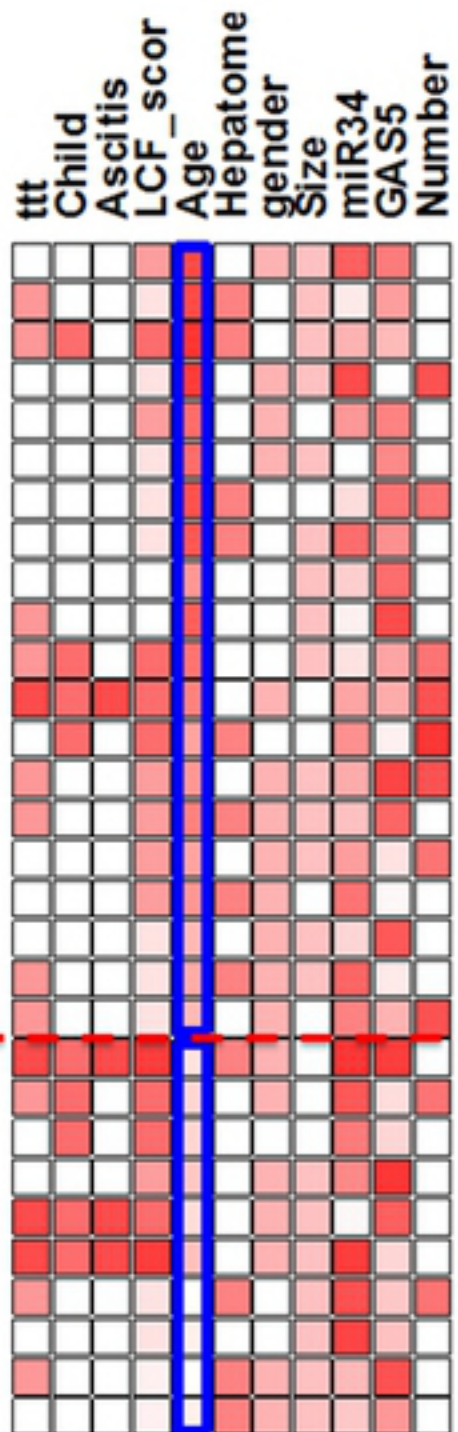
HCC patients

Information Remaining (%)

0 25 50 75 100



- H1
- H21
- H4
- H22
- H3
- H27
- H6
- H11
- H28
- H29
- H2
- H19
- H23
- H12
- H26
- H18
- H25
- H5
- H24
- H15
- H7
- H14
- H16
- H30
- H20
- H17
- H8
- H13
- H9
- H10



Old age

Young age